oxygen

MDPI

Article

Hydrogenation of Aromatic Ethers and Lactones: Does the Oxygen Functionality Really Improve the Thermodynamics of Reversible Hydrogen Storage in the Related LOHC Systems?

Riko Siewert [1,2], Artemiy A. Samarov [3], Sergey V. Vostrikov [4], Karsten Müller [1,2], Peter Wasserscheid [5] and Sergey P. Verevkin [1,2,4,*]

[1] Institute of Technical Thermodynamics, University of Rostock, 18059 Rostock, Germany; riko.siewert@uni-rostock.de (R.S.); karsten.mueller@uni-rostock.de (K.M.)
[2] Competence Centre °CALOR, Department Life, Light & Matter of the Faculty of Interdisciplinary Research, University of Rostock, 18059 Rostock, Germany
[3] Department of Chemical Thermodynamics and Kinetics, Saint Petersburg State University, Peterhof, 198504 Saint Petersburg, Russia; samarov@yandex.ru
[4] Engineering and Technology Department, Samara State Technical University, 443100 Samara, Russia; vosser@mail.ru
[5] Institute of Chemical Reaction Engineering, Friedrich-Alexander-Universität Erlangen-Nürnberg, Egerlandstr. 3, 91058 Erlangen, Germany; peter.wasserscheid@fau.de
* Correspondence: sergey.verevkin@uni-rostock.de

Abstract

Compounds known as liquid organic hydrogen carriers (LOHCs) offer a promising pathway for storing hydrogen. Beyond the use of pure hydrocarbons, the incorporation of oxygen atoms offers a way to modify thermodynamic properties and potentially improve suitability for hydrogen storage. This study explores the effect of oxygen functionalization in aromatic ethers and lactones on the reaction equilibrium of reversible hydrogenation. To address this question, reaction enthalpies and entropies are calculated using both experimental and theoretically determined pure substance data. The equilibrium position shift in the hydrogenation of furan derivatives has been shown to follow a similar trend to that of their hydrocarbon counterparts upon the addition of aromatic rings. This shift is, however, more pronounced in the case of the furan-based systems. The effect is reflected in increasing Gibbs reaction energies during the dehydrogenation process. Both the formation of lactones and the addition of a second ring to the furan core leads to a further increase in the Gibbs reaction energy. The highest value is observed for dibenzofuran, with a Gibbs reaction energy of 36.6 kJ·mol^{-1} at 500 K. These findings indicate that, from a thermodynamic perspective, hydrogen release is feasible at temperatures below 500 K, which is an important feature for the potential application as a hydrogen storage system.

Keywords: hydrogen storage; LOHC; enthalpies of phase transitions; enthalpy of formation; vapour pressure; structure–property correlation; quantum chemical calculations

Academic Editor: John T. Hancock

Received: 27 June 2025
Revised: 25 August 2025
Accepted: 26 August 2025
Published: 30 August 2025

Citation: Siewert, R.; Samarov, A.A.; Vostrikov, S.V.; Müller, K.; Wasserscheid, P.; Verevkin, S.P. Hydrogenation of Aromatic Ethers and Lactones: Does the Oxygen Functionality Really Improve the Thermodynamics of Reversible Hydrogen Storage in the Related LOHC Systems? *Oxygen* **2025**, *5*, 18. https://doi.org/10.3390/oxygen5030018

1. Introduction

Liquid organic hydrogen carrier systems featuring oxygen-based functionalities have been shown to deliver excellent hydrogen release efficiency at comparatively low temperatures, combined with characteristics that are advantageous for prospective technical applications [1]. As an example, benzophenone has been reported to undergo selective and complete hydrogenation to form di-cyclohexyl-methanol over Ru/Al_2O_3 catalysts

at a hydrogen pressure of 50 bar and temperatures between 90 and 180 °C. Hydrogen is released from di-cyclohexyl methanol at a temperature of 250 °C using Pt-based catalysts in order to recover benzophenone. This reversible process exhibits an excellent theoretical hydrogen storage capacity of 7.2 mass percent [2]. The positive outcome has encouraged additional studies on oxygen-containing hydrogen carrier materials [3]. The influence of oxygen-containing functional groups on the thermodynamic behaviour of hydrogenation and dehydrogenation reactions was examined for LOHC systems derived from methoxy-benzene, benzyl phenyl ether, diphenyl ether, dibenzyl ether, and various methoxy-naphthalenes. The resulting data were compared with corresponding values for structurally related hydrogen carriers based on benzene, naphthalene, and diphenylalkanes [3]. A noticeable reduction in both reaction enthalpy and Gibbs free energy was found for the dehydrogenation methoxy-naphthalenes and methoxy-benzene, which results in improved reaction conditions. Conversely, aromatic ether-based systems without these specific oxygen functionalities exhibited thermodynamic profiles largely matching their oxygen-free counterparts. These recent findings have enhanced the comprehension of the thermodynamic characteristics of LOHC materials. The investigation of the thermodynamic properties of hydrogenation/dehydrogenation reactions in LOHC systems with oxygen functions would need to be expanded to evaluate this interesting structure–property relationship for the screening of molecules suitable for practical applications. Currently, knowledge about the reaction-thermodynamic properties for this potential class of hydrogen carrier is limited. To extend the scientific understanding of these systems, the in-depth investigation of its thermochemistry is required.

In order to simplify the evaluation and comparison of thermodynamic data for LOHC systems, it makes sense to select a few indicators that relate to physical and chemical properties and are relevant for comparison and practical implementation. The most obvious of them are the hydrogen storage capacity (e.g., in % mass) and the equilibrium temperature, T_{eq}:

$$T_{\mathrm{eq}} = \frac{\Delta_r H^{\mathrm{o}}_{\mathrm{m}}}{\Delta_r S^{\mathrm{o}}_{\mathrm{m}}} \quad (1)$$

where $\Delta_r H^o_m$ is the standard molar reaction enthalpy and $\Delta_r S^o_m$ is the standard molar reaction entropy. This temperature is considered the potential optimum reaction temperature for a hydrogenation/dehydrogenation process. Generally, the temperature should be as low as possible. The reaction enthalpy values are also considered a valuable indicator, which should be as low as possible, since lower values reduce the temperature level needed for dehydrogenation. An example for the application of the indicators is shown in Figure 1, where the oxygen functionality is directly bound to the benzene ring and compared with similarly structured hydrocarbon systems.

Obviously, introducing oxygen into the aromatic system can only reduce the hydrogen storage capacity, but in return, the T_{eq} value in the methoxy-benzene/methoxy-cyclohexane system drops to 554 K compared to 569 K in the benzene/cyclohexane system. An analogous trend can be observed in the reaction enthalpy in the methoxy-benzene/methoxy-cyclohexane system compared to the benzene/cyclohexane system (see Figure 1).

From a structural point of view, the oxygen functionality cannot only be bound to the aromatic ring of promising LOHC structures as shown in Figure 1, but also as part of bicyclic molecules in which the oxygen is part of a five-membered ring (e.g., benzofuran, dibenzofuran, indanol, indanone, etc.) or a six-membered ring (e.g., chromene, isochromene, tetralones, tetralols, etc.). The strain on the corresponding rings can certainly influence the thermodynamic properties of these auspicious LOHC compounds. Therefore, the current study investigates whether adding oxygen-based functional groups to aromatic bi- and tricyclic molecules with a five-membered ring (see

Figure 2) improves the thermodynamic characteristics of hydrogen storage in comparison to analogous LOHC materials that do not contain oxygen. Bi- and tricyclic molecules are also technically particularly interesting as they exhibit lower volatilities than their smaller monocyclic counterparts. This simplifies the purification of the hydrogen and recovery of the carrier after hydrogen release.

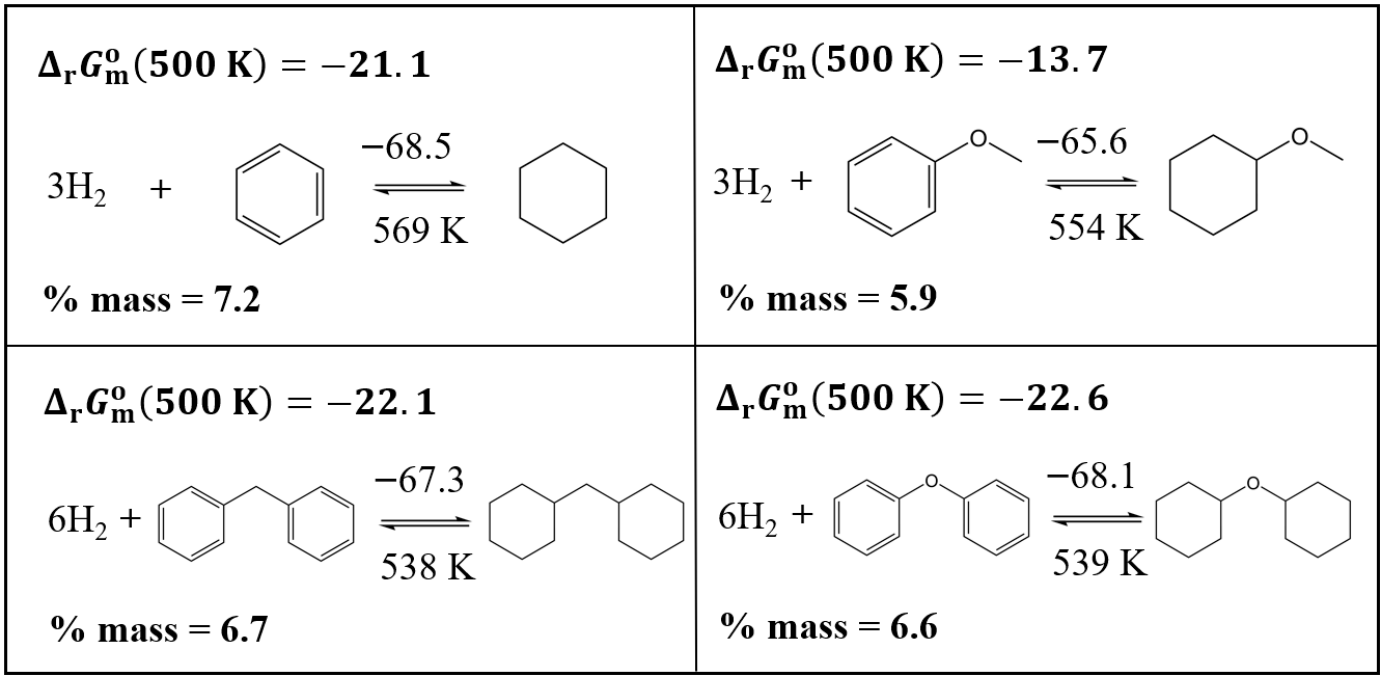

Figure 1. The comparison of reaction enthalpies, ($\Delta_r H^o_m$ per H2, given in kJ·mol^{-1}), equilibrium temperatures (T_{eq} in K), gravimetric capacities (in % mass), and Gibbs energies ($\Delta_r G^o_m$ in kJ·mol^{-1}) of hydrogenation reactions of C, H and C, H, O containing LOHC.

It is well established that the hydrogenation of LOHC systems is a chemically reversible process. However, the optimisation of the experimental reaction conditions is essential to achieve sufficient hydrogen release at moderate temperatures. This work compiles and assesses thermodynamic data on hydrogen-lean (HL) forms of the LOHC systems (refer to Figure 2) through empirical evaluation and quantum chemical calculations. Since experimental data for partially and fully hydrogenated aromatics (see Figure 2) are practically non-existent in the literature, the thermodynamic data for these hydrogen-rich (HR) counterparts of the LOHC systems were derived using specially developed empirical correlations and methods as well as high-level quantum chemical calculations and finally are recommended for chemical engineering calculations.

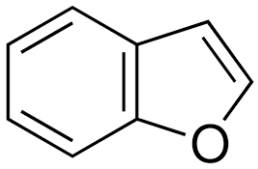

2,3-benzofuran, 271-89-6

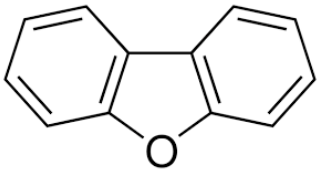

dibenzofuran, 132-64-9

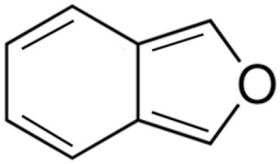

isobenzofuran, 270-75-7

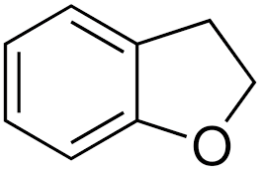

2,3-dihydro-benzofuran
496-16-2

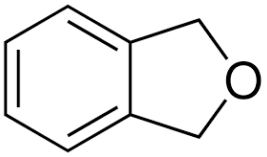

1,3-dihydro-isobenzofuran,
496-14-0

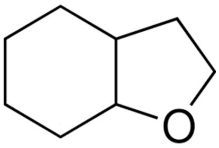

8H-benzofuran
13054-97-2

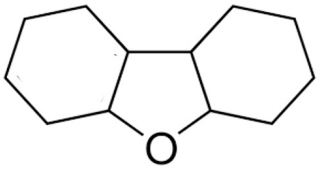

12H-dibenzofuran
13054-98-3

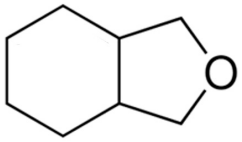

10H-isobenzofuran
4743-54-8

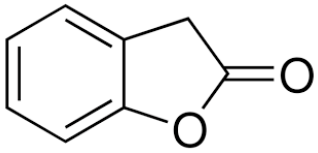

2-coumaranone, 553-86-6

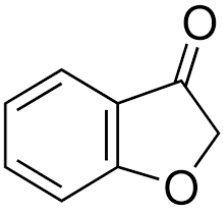

3-coumaranone, 7169-34-8

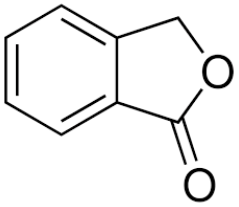

phthalide, 87-41-2

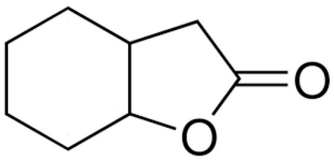

6H-2-coumaranone
6051-03-2

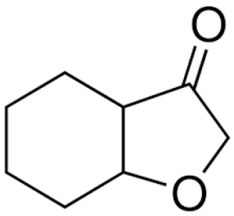

6H-3-coumaranone
1206676-08-5

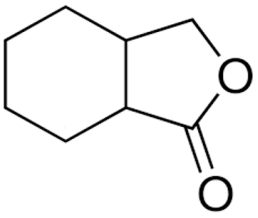

6H-phthalide
2611-01-0

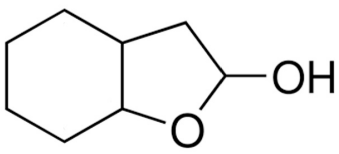

8H-benzofuran-2-ol
36871-99-5

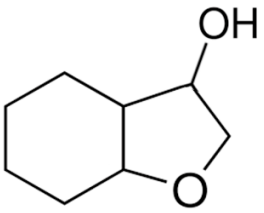

8H-benzofuran-3-ol
99769-38-7

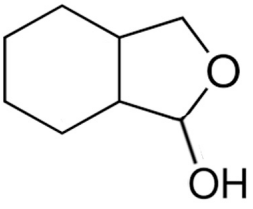

8H-benzofuran-1-ol
59901-42-7

Figure 2. Structures of aromatic and aliphatic compounds with oxygen functionalities studied in this work.

2. Approach

As a rule for our considerations, LOHC hydrogenation and dehydrogenation reactions proceed in the liquid phase. Unfortunately, data on the enthalpies of formation for the HL and HR species are not always found in the literature, or the available data originate from a single measurement and therefore need to be validated. Admittedly, modern quantum chemical (QC) computations now provide chemically accurate gas-phase enthalpies of formation, $\Delta_f H_m^o$(g, 298.15 K), and absolute entropies, S_m^o(g, 298.15 K) [4].

In the first step, high-level QC methods were applied to calculate the gas-phase formation enthalpies and absolute entropies of the substances involved in the hydrogenation/dehydrogenation processes.

In Step II, the combination of experimental vapour pressures and empirical methods enabled the assessment of reliable vaporisation enthalpies $\Delta_l^g H_m^o$(298.15 K), and vaporisation entropies, $\Delta_l^g S_m^o$(298.15 K), which were required to derive the enthalpies of formation in the liquid phase, $\Delta_f H_m^o$(liq, 298.15 K), according to Equation (2):

$$\Delta_f H_m^o(\text{liq}, 298.15\ \text{K}) = \Delta_f H_m^o(\text{g}, 298.15\ \text{K})_{\text{QC}} - \Delta_l^g H_m^o(298.15\ \text{K}) \quad (2)$$

and the liquid phase absolute entropies, S_m^o(liq, 298.15 K) according to Equation (3):

$$S_m^o(\text{liq}, 298.15\ \text{K}) = S_m^o(\text{g}, 298.15\ \text{K}) - \Delta_l^g S_m^o(298.15\ \text{K}) \quad (3)$$

In Step III, the $\Delta_f H_m^o$(liq, 298.15 K) and S_m^o(liq, 298.15 K) values were used to derive $\Delta_r H_m^o$(liq, 298.15 K) and $\Delta_r S_m^o$(liq, 298.15 K) and used to calculate the Gibbs free energies $\Delta_r G_m^o$(liq, 298.15 K), according to Equation (4):

$$\Delta_r G_{\text{m}}^{\text{o}} = \Delta_r H_{\text{m}}^{\text{o}} - T \times \Delta_r S_{\text{m}}^{\text{o}} \quad (4)$$

and finally to calculate the equilibrium temperatures for the hydrogenation/dehydrogenation reactions with the compounds given in Figure 2 and to perform a thermodynamic analysis of the LOHC system of interest. These three stages form the overall framework aim to assess the impact and practical applications of adding oxygen functional groups to aromatic ether-based LOHC systems compared to similarly structured aromatics.

3. Results and Discussion

3.1. Step I: Quantum Chemical Calculations of the Gas-Phase Enthalpies of Formation

Aromatic ethers (see Figure 2) are generally rigid molecules, but aliphatic ethers (the partially or completely hydrogenated products of the species shown in Figure 2) display flexibility and exist as conformer mixtures in the gas phase. A careful conformational analysis was performed using CREST version 3.0.2 software [5]. The G3MP2 method implemented in the Gaussian 16 software [6] was used to calculate the energies E_0 and total enthalpies H_{298} of the most stable conformers. The calculated H_{298} enthalpies were converted to the standard molar enthalpies of formation based on the conventional atomisation (AT) procedure [7] (e.g., for 2,3-benzofuran):

$$\text{C}_8\text{H}_6\text{O} \rightarrow 8 \times \text{C} + 6 \times \text{H} + 1 \times \text{O} \quad (5)$$

The quantum chemical G3MP2 calculation results for the HL and HR forms of the LOHC systems are compiled in Table S1 (column 3).

Among various reaction types like isogyric, isodesmic, and homodesmotic, the AT reaction was preferred, as it provides the least biassed conversion of H298 enthalpies to standard molar enthalpies of formation [7]. One key benefit of the AT reaction lies in

the precise quantification of atomic enthalpies. Conversely, the enthalpies of formation for the different molecules involved in the previously mentioned reactions are subject to considerable uncertainties. However, it has also been shown in references [7,8] that the G3MP2 results and AT reactions, $\Delta_f H^o_m$(g, AT), exhibit a slight but discernible deviation from values derived experimentally. Using a reference set of molecules with well-known experimental formation enthalpies, $\Delta_f H^o_m(\mathrm{g})_{\mathrm{exp}}$, (see Table S1) allows for a correction of QC and experimental data. Thus, a correlation is established between the $\Delta_f H^o_m$(g, AT) values and the experimental results. The following equation was used to obtain the "corrected" atomisation results for the aromatic ethers (see Figure 2) and their hydrogenated forms:

$$\Delta_f H^o_m(\mathrm{g})_{\mathrm{G3MP2}}/\mathrm{kJ{\cdot}mol^{-1}} = 1.0091 \times \Delta_f H^o_m(\mathrm{g})_{\mathrm{AT}} + 10.9 \text{with } \mathrm{R^2} = 0.9993 \quad (6)$$

The enthalpies derived from the corrected atomisation reaction calculations are shown in Table 1, column 2, and compared with the QC results from other studies (see Table 1, columns 3 and 4).

Table 1. Comparison of the quantum chemical and experimental enthalpies of formation of the HL compounds (at T = 298.15 K and p° = 0.1 MPa, in kJ·mol^{-1}) [a].

Compound	$\Delta_f H^o_m$(g) [b] G3MP2/AT	$\Delta_f H^o_m$(g) [c] G3MP2//B3LYP	$\Delta_f H^o_m$(g) [d] G3MP2	$\Delta_f H^o_m(\mathrm{g})_{\mathrm{QC}}$ [e]	$\Delta_f H^o_m$(g) [f] (exp)
2,3-benzofuran	17.2	16.6		16.9	13.9 ± 0.7
2,3-dihydrobenzofuran	−47.1	−45.5		−46.3	−46.7 ± 0.9
isobenzofuran	67.3				79.3 ± 4.1
1,3-dihydro-isobenzofuran	−26.3	−26.0		−26.1	−30.6 ± 1.2
dibenzofuran	50.1	48.9		49.5	52.9 ± 0.7
2-coumaranone	−222.7	−217.5 [d]	−218.1	−218.7	(−210.8 ± 4.0)
3-coumaranone	−166.3	−162.1 [d]	−162.3	−162.9	−168.8 ± 2.4
phthalide	−224.1	−220.4 [d]	−220.7	−221.4	−220.6 ± 2.8

[a] Uncertainties in this table are expressed as two times the standard deviation. [b] From Table S1, column 5, calculated in this work by G3MP2 and the atomization reaction, corrected according to Equation (6). [c] From Table S2, column 5, calculated by Notario et al. [9] using the G3MP2//B3LYP method and the "corrected" atomization reaction. [d] Calculated by Sousa et al. [10] using the G3MP2 method and the well-balanced reactions shown in Figure S2. [e] The average value determined from the data in columns 2 to 4. [f] The available experimental results, evaluated in this work and shown in Table 2, column 5. The value in parentheses seems to be in error.

Table 2. Comparison of experimental and theoretical thermochemical data for the hydrogen lean (HL) compounds (at T = 298.15 K, p° = 0.1 MPa, in kJ·mol^{-1}) [a].

Compounds	$\Delta_f H^o_m$(liq or cr)	$\Delta^{\mathrm{g}}_{\mathrm{l/cr}} H^o_m$ [b]	$\Delta_f H^o_m(\mathrm{g})_{\mathrm{exp}}$ [c]	$\Delta_f H^o_m(\mathrm{g})_{\mathrm{QC}}$ [d]
2,3-benzofuran [271-89-6] (liq)	−34.8 ± 0.7 [11] −35.3 ± 1.6 [12] **−34.9 ± 0.6**	**48.4 ± 0.4**	**13.9 ± 0.7**	16.9 ± 2.9
2,3-dihydro-benzofuran [496-16-2] (liq)	−99.8 ± 0.7 [11] −100.6 ± 1.9 [13] **−99.9 ± 0.8**	**53.2 ± 0.3**	**−46.7 ± 0.9**	−46.3 ± 2.9
1,3-dihydro-isobenzofuran [496-14-0] (liq)	−83.8 ± 0.9 [14]	53.2 ± 0.8	−30.6 ± 1.2	−26.1 ± 2.9
dibenzofuran [132-64-9] (cr)	−29.1 ± 0.6 [15]	82.0 ± 0.3 [16]	52.9 ± 0.7	49.5 ± 2.9
fluorene [86-73-7] (cr)	89.9 ± 1.4 [17]	86.1 ± 0.1 [18]	176.0 ± 1.4	-
2-coumaranone [553-86-6] (cr)	(−292.4 ± 3.7) [10]	81.6 ± 1.4 [f]	(−210.8 ± 4.0)	**−218.7 ± 1.9**

Table 2. *Cont.*

Compounds	$\Delta_f H_m^o$(liq or cr)	$\Delta_{l/cr}^{g} H_m^o$ [b]	$\Delta_f H_m^o(g)_{exp}$ [c]	$\Delta_f H_m^o(g)_{QC}$ [d]
3-coumaranone [7169-34-8] (cr)	−254.9 ± 2.0 [10]	86.1 ± 1.4 [g]	−168.8 ± 2.4	−162.9 ± 1.9
phthalide [87-41-2] (cr)	(−366 ± 10) [19] **−312.4 ± 1.5** [20]	**92.0 ± 2.2** [h]	**−220.6 ± 2.8**	−221.4 ± 2.3

[a] Uncertainties correspond to expanded uncertainties of the mean (0.95 level of confidence). The values highlighted in bold were used for further thermochemical calculations. The values in brackets were considered unreliable. [b] The evaluated data from Table 3. [c] Sum of columns 2 and 3. [d] The averaged quantum chemical results from Table 1, column 6. [e] For 2-coumaranone, the sublimation enthalpy, $\Delta_{cr}^{g} H_m^o$(298.15 K) = 81.6 ± 1.4 kJ·mol^{-1} was calculated as a sum of the enthalpy of vaporisation $\Delta_{l}^{g} H_m^o$(298.15 K) = 64.8 ± 1.0 kJ·mol^{-1} [Table 3] and the enthalpy of fusion $\Delta_{cr}^{l} H_m^o$(298.15 K) = 16.8 ± 1.1 kJ·mol^{-1} [Table S3]. [f] For 3-coumaranone, the sublimation enthalpy, $\Delta_{cr}^{g} H_m^o$(298.15 K) = 86.1 ± 1.4 kJ·mol^{-1} was calculated as the average from $\Delta_{cr}^{g} H_m^o$(298.15 K) = 85.8 ± 1.7 kJ·mol^{-1} [10] and the sublimation enthalpy $\Delta_{cr}^{g} H_m^o$(298.15 K) = 86.8 ± 2.8 kJ·mol^{-1} calculated as the sum of enthalpy of vaporisation $\Delta_{l}^{g} H_m^o$(298.15 K) = 68.8 ± 2.3 kJ·mol^{-1} [Table 3] and the enthalpy of fusion $\Delta_{cr}^{l} H_m^o$(298.15 K) = 18.0 ± 1.6 kJ·mol^{-1} [Table S3]. [g] For phthalide, the sublimation enthalpy, $\Delta_{cr}^{g} H_m^o$(298.15 K) = 92.0 ± 2.2 kJ·mol^{-1} was calculated as the average from $\Delta_{cr}^{g} H_m^o$(298.15 K) = 88.4 ± 4.4 kJ·mol^{-1} [20] and the sublimation enthalpy $\Delta_{cr}^{g} H_m^o$(298.15 K) = 93.2 ± 2.8] kJ·mol^{-1} calculated as the sum of the enthalpy of vaporisation $\Delta_{l}^{g} H_m^o$(298.15 K) = 76.3 ± 2.5 kJ·mol^{-1} [Table 3] and the enthalpy of fusion $\Delta_{cr}^{l} H_m^o$(298.15 K) = 16.9 ± 1.2 kJ·mol^{-1} [Table S3].

Table 3. Compilation of the standard molar enthalpies of vaporisation of HL and HR counterparts of LOHC systems (in kJ·mol^{-1}).

Compounds	Method [a]	*T*-Range/ K	$\Delta_{l}^{g} H_m^o$ T_{av}	$\Delta_{l}^{g} H_m^o$ 298.15 K [b]	
2,3-benzofuran [271-89-6]	n/a	323–403	45.0 ± 1.5	47.9 ± 1.6	[21]
	E	273.2–488.1	45.1 ± 0.1	48.0 ± 0.6	[11]
	T	278.7–313.4	49.0 ± 0.4	48.8 ± 0.6	[12]
				48.4 ± 0.4 [c]	average
	J_x			49.4 ± 1.0	Table 4
2,3-dihydro-benzofuran [496-16-2]	E	285.0–503.2	48.7 ± 0.1	53.0 ± 0.9	[11]
	T	278.7–333.0	52.7 ± 0.2	53.2 ± 0.4	[13]
	BP	341–465	47.8 ± 0.8	53.2 ± 1.3	Table S4
				53.2 ± 0.3 [c]	
	J_x			52.7 ± 1.0	Table 4
	CP			52.5 ± 1.5	Figure 3
1,3-dihydro-isobenzofuran [496-14-0]	E	285.0–503.2	48.9 ± 0.1	53.3 ± 0.9	[14]
phthalan	CGC	298		52.7 ± 2.9	[22]
	BP	318–465	48.0 ± 1.1	53.1 ± 1.5	Table S4
				53.2 ± 0.8 [c]	average
	J_x			52.6 ± 1.0	Table 4
8H-octahydro-benzofuran [13054-97-2]	*BP*	337–446	44.5 ± 0.8	48.8 ± 1.9	Table S4
	T_b			48.8 ± 1.5	Equation (7)
				48.8 ± 1.2 [c]	average
	CP			49.0 ± 1.5	Figure 3
	CP			48.3 ± 1.5	Figure S3
	CP			48.4 ± 1.5	Figure 3
	GA			48.9 ± 1.5	Figure S3

Table 3. *Cont.*

Compounds	Method [a]	*T*-Range/ K	$\Delta_l^g H_m^o$ T_{av}	$\Delta_l^g H_m^o$ 298.15 K [b]	
8H-octahydro-isobenzofuran [4743-54-8]	*BP*	324–453	43.8 ± 0.8	48.1 ± 1.2	Table S4
	T_b			49.9 ± 1.5	Equation (7)
				48.8 ± 0.9 [c]	average
	CP			48.8 ± 1.5	Figure 3
	CP			48.3 ± 1.5	Figure 3
	CP			48.3 ± 1.5	Figure S4
	GA			48.8 ± 1.5	Figure S4
12H-dodecahydro-dibenzofuran [13054-98-3]	*BP*	381–532	52.2 ± 1.4	63.8 ± 2.7	Table S4
2(3H)-benzofuranone [553-86-6]	PhT	298		61.9 ± 2.0	Table S3
2-coumaranone	*BP*	384–521	57.0 ± 1.8	65.3 ± 2.4	Table S4
	J_x			65.7 ± 1.5	Table S7
	J_x			65.7 ± 2.0	Table S8
	CP			67.3 ± 1.5	Figure S5
	CP			66.2 ± 1.5	Figure S5
				65.7 ± 0.7	average
benzofuran-3(2H)-one [7169-34-8]	PhT	298		67.8 ± 2.3	Table S3
3-coumaranone	*BP*	425–551	60.3 ± 1.5	68.8 ± 2.3	Table S4
	CP			66.7 ± 1.5	Figure S6
	CP			67.3 ± 1.5	Figure S6
	CP			65.5 ± 1.5	Figure S6
				66.9 ± 0.8 [c]	average
2-benzofuran-1(3H)-one [87-41-2]	n/a	368.7–563.0	58.7 ± 1.5	(66.9 ± 2.2)	[23]
phthalide	PhT	298		71.5 ± 4.6	Table S3
	BP	346–563	69.0 ± 2.0	76.3 ± 2.5	Table S4
	CP			74.7 ± 1.5	Figure S7
	CP			75.4 ± 1.5	Figure S7
	CP			73.6 ± 1.5	Figure S7
				74.7 ± 0.8 [c]	average
6H-hexahydro-2-coumaranone [6051-03-2]	*BP*	327–537	56.3 ± 1.7	64.3 ± 2.3	Table S4
6H-hexahydro-3-coumaranone [1206676-08-5]	*BP*	353–626	54.2 ± 0.7	65.2 ± 2.3	Table S4
	CP			62.5 ± 1.5	Figure S8
	CP			63.0 ± 1.5	Figure S8
	CP			62.2 ± 1.5	Figure S8
				62.9 ± 0.8 [c]	average
6H-hexahydro-phthalide [2611-01-0]	*BP*	337–503	72.3 ± 0.8	77.6 ± 1.3	Table S4
octahydro-benzofuran-2-ol [36871-99-5]	*CP*			66.5 ± 2.0	Figure S9
	CP			67.2 ± 2.0	Figure S9
				66.9 ± 1.4 [c]	average
8H-octahydro-benzofuran-3-ol [99769-38-7]	*BP*	354–513	63.8 ± 1.6	73.2 ± 2.5	Table S4
	CP			73.0 ± 2.0	Figure S9
	CP			73.5 ± 2.0	Figure S9
				73.2 ± 1.2 [c]	average

Table 3. *Cont.*

Compounds	Method [a]	*T*-Range/ K	$\Delta_l^g H_m^o$ T_{av}	$\Delta_l^g H_m^o$ 298.15 K [b]	
8H-octahydro-isobenzofuran-1-ol	*CP*			66.7 ± 2.0	Figure S9
[59901-42-7]	*CP*			66.5 ± 2.0	Figure S9
				66.6 ± 1.4 [c]	average
methoxy-benzene [100-66-3]				46.4 ± 0.2	[24]
methoxy-cyclohexane [931-56-6]				43.0 ± 0.5	[25]

[a] Methods: n/a = method is not available; T = transpiration method; E = ebulliometry; T_b = from the correlation with the normal boiling temperatures; PhT = from the consistency of phase transitions (see Table S3); *BP* = estimated from boiling points at different pressures (see Table S4); J_x = calculated from the correlation with the Kovats retention indices; *CP* = calculated according to the centrepiece approach (see text). [b] Using vapour pressure data from the literature, Equations (S2) and (S3) alongside heat capacity differences from Table S5 were applied to determine the enthalpies of vaporisation at 298.15 K. Expanded uncertainties $U(\Delta_l^g H_m^o)$ at the 0.95 confidence level include contributions from fitting errors and temperature adjustments to the reference temperature. The temperature adjustment accounts for about 20% of the total uncertainty. [c] Bolded weighted mean values, where uncertainties serve as weights, are suggested for further calculations.

Notario et al. [9] calculated the enthalpies of formation of all aromatic ethers shown in Figure 2 using the G3MP2//B3LYP method and the atomisation reaction. The original atomisation enthalpies were corrected as shown in Table S2, and the resulting "corrected" enthalpies of formation (see Table 1, column 3) agree with our G3MP2 calculations (see Table 1, column 2).

Sousa et al. [10] calculated the enthalpies of formation of 2-cumarone, 3-cumarone and phthalide using the G3MP2 and G3MP2/B3LYP methods and using 10 different well-balanced reactions, which are shown in Figure S2. It should be noted that the selection of the appropriate reactions cannot be considered optimal, as the fluctuations in the resulting $\Delta_f H_m^o(g)_{G3MP2}$ for each aromatic lactone were unacceptably large (e.g., for phthalide, they ranged between −210.0 and -230.6 kJ·mol^{-1}). Surprisingly, despite this variation, the values averaged by Sousa et al. [10] (see Table 1, column 4) agree well with our G3MP2 calculations (see Table 1, column 2) and with the "corrected" results of Notario et al. [9] (see Table 1, column 3). The weighted average value $\Delta_f H_m^o(g)_{QC}$, which was determined from the data in columns 2, 3, and 4 (Table 1, column 5) using the uncertainty as a weighting factor, was recommended as reliable and compared with the available experimental results evaluated in this work and presented in Table 2, column 5.

With the exception of 2-coumaranone, the quantum chemical and experimental gas phase enthalpies of formation of the compounds listed in Table 2 agree well within the uncertainties specified for these values. In order to find an explanation for the observed discrepancy, the experimental details of the combustion experiments with 2-coumaranone were analysed as described in the original paper [10], as follows. The combustion experiments with 2-coumaranone and 3-coumaranone were carried out using a micro-bomb calorimeter with sample masses of approximately 20 mg. The samples of 2-coumaranone were burned in pellet form, which were enclosed in Melinex bags due to the high volatility of the compound. Moreover, incomplete combustion was observed for 2-coumaranone. Even when an appropriate correction for the formation of carbon soot was made by the authors, the reliability of the experimental enthalpy of formation for this compound remains questionable.

The good agreement between the quantum chemical and experimental gas phase enthalpies of formation of the compounds listed in Table 2 can be regarded as mutual validation of both data sets, and these data have been recommended for further thermodynamic calculations.

3.2. Step II: Evaluation of the Thermodynamic Functions of Vaporisation

3.2.1. Absolute Vapour Pressures and Vaporisation Enthalpies

The primary vapour pressure–temperature dependencies for aromatic ethers and lactones as well as their hydrogenated counterparts were compiled from the literature and uniformly fitted using a three-parameter equation (details available in the ESI). Based on these values, the vaporisation enthalpies at the corresponding temperatures T_{av} (average temperature of the measurement interval) were derived and adjusted to the reference temperature T = 298.15 K for comparison. The resulting $\Delta_l^g H_m^o$ (298.15 K) values for the compounds of interest are summarised and compared in Table 3.

The $\Delta_l^g H_m^o$ (298.15 K) values for 2,3-benzofuran, 2,3-dihydrobenzofuran, and 1,3-dihydroisobenzofuran (phthalane), which were determined using various techniques, are very consistent, and a weighted average value was determined for each compound and recommended for thermochemical calculations.

For 2-coumaranone, 3-coumaranone, and phthalide, only the sublimation enthalpies were measured directly [10,20] using drop calorimetry. The corresponding enthalpies of vaporisation, $\Delta_l^g H_m^o$ (298.15 K), were derived in this work using fusion enthalpies (see Table S3). These values still need to be validated, especially for phthalide, where $\Delta_l^g H_m^o$ (298.15 K) = 71.5 ± 4.6 kJ·mol^{-1} (Table 3) deviates significantly from the value of $\Delta_l^g H_m^o$ (298.15 K) = 66.9 ± 2.2 kJ·mol^{-1} (see Table 3) derived from the Antoine equation coefficients given in the comprehensive compilation by Stephenson and Malanowski [21].

For most hydrogenated aromatic ethers, no consistent vapour pressure data sets are available. Nevertheless, boiling point measurements of the desired aliphatic cyclic ethers at different reduced pressures have been documented (compiled in Table S4). These measurements may assist in filling the gaps in thermodynamic information. Typically, such boiling point data are derived from distillation experiments on reaction mixtures post-synthesis and are primarily used for compound identification. In these experiments, pressures are often measured with uncalibrated manometers, and temperatures are recorded with an uncertainty of several degrees. In prior research, such as on methyl-biphenyls [26]) it has been shown that meaningful trends may be extracted even when using data of limited precision. This general conclusion is also applicable for these aromatic ethers [3]. We therefore carefully collected the available boiling points at reduced pressures for 2,3-benzofuran, 2,3-dihydrobenzofuran, 2 coumaranone, 3-coumaranone phthalide, and their hydrogenated products, and used these data to calculate the vaporisation enthalpies $\Delta_l^g H_m^o$(298.15 K) and vaporisation entropies $\Delta_l^g S_m^o$(298.15 K) required for the thermodynamic analysis of the hydrogenation/dehydrogenation reactions relevant to this work. The enthalpies of vaporisation derived from the approximation of the boiling points at reduced pressures selected in Table S4 are given in Table 3 as *BP*.

3.2.2. Validation of Vaporisation Enthalpies by Structure–Property Correlations

A key aspect of physical chemistry is understanding structure–property relationships. New data that are consistent with existing trends can be confidently applied, while inconsistent results warrant the repetition of measurements. Consequently, prior to utilising $\Delta_l^g H_m^o$(298.15 K) values from individual experiments or boiling point data, it is recommended to verify them using structure–property correlation analyses. For instance, correlations between the enthalpy of vaporisation and normal boiling points (T_b) enable a simple plausibility test.

For example, in our recent work [25], we established a reliable $\Delta_l^g H_m^o$(298.15 K) − T_b correlation for a large series of aliphatic ethers:

$$\Delta_l^g H_m^o(298.15\ \text{K})/\text{kJ·mol}^{-1} = 0.1592 \times T_b - 22.2 \text{ with } R^2 = 0.9930 \quad (7)$$

This correlation was applied to calculate $\Delta_l^g H_m^o$(298.15 K) values for octahydrobenzofuran and octahydro-isobenzofuran and the results (shown in Table 3 as T_b) showed good agreement with enthalpies of vaporisation estimated from *BP* approximation.

A valuable option called the "centrepiece approach", which is closely related to group additivity (GA) methods, has been developed in a series of our recent work on the correlation of structures and thermodynamic properties [27]. The "centrepiece approach" is an empirical method for assessing the thermochemical properties (e.g., enthalpies of vaporisation, enthalpies of formation, etc.) of organic molecules with improved accuracy and efficiency. It involves selecting a well-characterised "centrepiece" molecule, typically a structurally similar compound with reliable properties, as a starting point. The target molecule is then analysed by calculating the relative differences in thermochemical properties between it and the "centrepiece molecule" (for more details, see the ESI). This differential approach helps to reduce systematic errors and improve the reliability of predictions, especially for large or complex organic molecules. Examples of calculations using the "centrepiece approach" for LOHC pairs are shown in Figure 3.

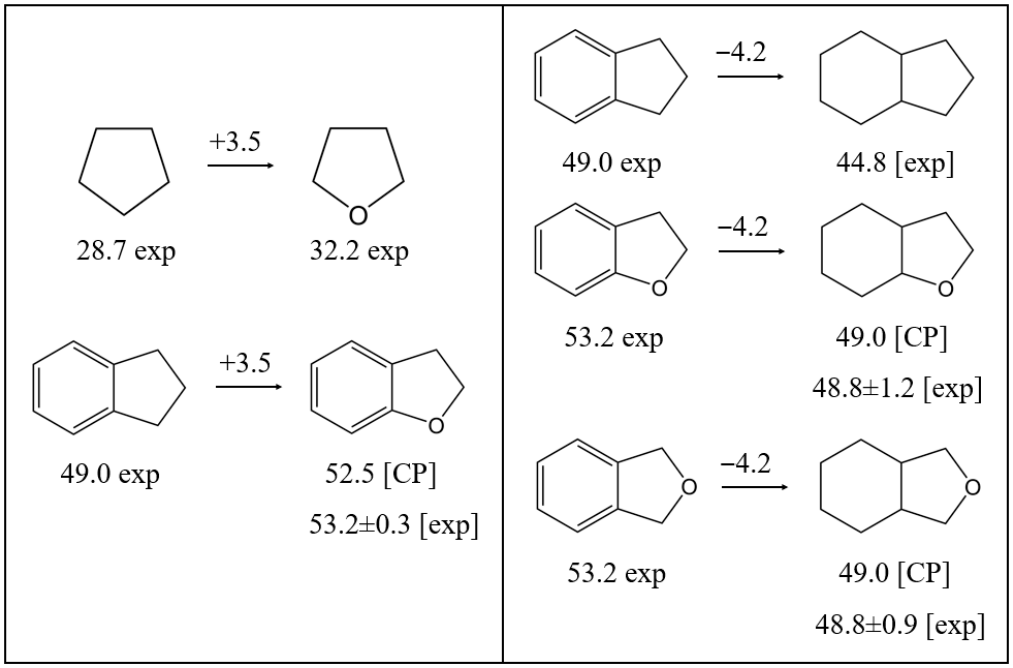

Figure 3. Calculating the enthalpy of vaporisation, $\Delta_l^g H_m^o$ (298.15 K)/kJ·mol^{-1} of 2,3-dihydrobenzofuran (**left**) and 8H-benzofuran or 8H-isobenzofuran (**right**) using the "centrepiece approach" (*CP*). The numerical values of enthalpies of vaporisation required for the calculations are given in Table S6.

Indeed, to calculate the enthalpy of vaporisation of 2,3-dihydrobenzofuran, it is logical to start with indane as the "centrepiece" molecule that is structurally most similar to 2,3-dihydrobenzofuran. To assess the enthalpy contribution for the exchange of the CH_2 fragment in the five-membered ring of indane with oxygen, the difference between the enthalpy of vaporisation of tetrahydrofuran and cyclopentane of Δ_O = 3.5 kJ·mol^{-1} was calculated (see Figure 3, left) and assumed to be equal to the value for the indane/2,3-dihydrobenzofuran pair. The latter contribution of 3.5 kJ·mol^{-1} was added to the reliable enthalpy of vaporisation of indane, $\Delta_l^g H_m^o$(298.15 K) = 49.0 ± 0.5 kJ·mol^{-1} [Table S6], and the empirical *CP* value of 52.5 kJ·mol^{-1} derived in this way agrees well with the experimental result of $\Delta_l^g H_m^o$(298.15 K) = 53.2 ± 0.2 kJ·mol^{-1} [Table 3].

The same "centrepiece" molecule indane was used to estimate the vaporisation enthalpies of 8H-benzofuran or 8H-isobenzofuran as fully hydrogenated counterparts of

2,3-dihydrobenzofuran and 1,3-dihydro-isobenzofuran (phthalan) (see Figure 3, right). In this case, it was assumed that the difference in the enthalpy of vaporisation of indane and 8H-indene (CAS 3296-50-2) is $\Delta_{(6+5)} = -4.2$ kJ·mol^{-1} and it is equal for all types of combinations of 6 + 5-membered rings. Based on this assumption and using the vaporisation enthalpies of 2,3-dihydrobenzofuran and phthalan given in Table 3, the missing vaporisation enthalpies for 8H-benzofuran or 8H-isobenzofuran were estimated. The latter results agree very well with the values determined using other methods (see Table 3).

In this work, the "centrepiece approach" was used to estimate the $\Delta_l^g H_m^o$(298.15 K) values for all partially and fully hydrogenated molecules in Figure 2. The "stepwise" estimates are documented in Figures S3–S10, and the final results are summarised in Table 3 with the notation *CP* ("centrepiece").

The bicyclic and polycyclic fully hydrogenated compounds shown in Figure 2 are general "hydrogen-rich" products of reversible hydrogenation/dehydrogenation reactions with LOHC. Admittedly, thermochemical data for this type of organic molecule are almost completely lacking in the literature. In this context, it is important to test various structure–property relationships in order to obtain reliable estimates for the vaporisation enthalpies of such cyclic molecules.

Another highly valuable tool for organic physical chemistry are group additivity (GA) methods. The approach resembles the concept of a Lego box, assembling a molecule's property from individual building blocks that provide numerical contributions to the total value. Nowadays, a comprehensive set of GA methods is available for the major classes of organic compounds [28,29].

The group contributions applied here to estimate thermodynamic properties are presented in Table S9. However, conventional GA approaches are known to face challenges with cyclic structures. To overcome this disadvantage, we have developed some additional cyclic increments, e.g., the methylene fragment in the five-membered aliphatic ring $[CH_2]_5$ and the six-membered aliphatic ring $[CH_2]_6$ or the oxygen atom $[O]_5$ incorporated into the five-membered ring. The numerical values for these new increments are also given in Table S9 and have significantly improved the prediction quality, as shown in Figure S3 using the example of 8H-benzofuran. The sum of the required increments for 8H-benzofuran yields an estimated value of $\Delta_l^g H_m^o$(298.15 K) = 48.9 ± 1.5 kJ·mol^{-1} [Figure S3], which, within the specified uncertainties, is hardly distinguishable from the result of the BP method $\Delta_l^g H_m^o$(298.15 K) = 48.8 ± 1.9 kJ·mol^{-1} [Table 3]. The vaporisation enthalpies estimated using the group-additivity contributions from Table S9 are given as *GA* values in Table 3.

An additional option to overcome the difficulties with the prediction of vaporisation enthalpies of a cyclic molecule is to combine the "centrepiece approach" with the group-additivity contributions from Table S9. Such an example is shown in Figure 4 for the calculation of the enthalpy of vaporisation, $\Delta_l^g H_m^o$(298.15 K) of 8H-benzofuran using data for 8H-indene.

The reliable vaporisation enthalpy, $\Delta_l^g H_m^o$(298.15 K) = 44.8 ± 1.3 kJ·mol^{-1} [Table S6], available for 8H-indene is a suitable "centrepiece" molecule in which replacing the cyclic hydrocarbon contribution $[CH_2]_5$ with the cyclic oxygen contribution $[O]_5$ given in Table S9 directly leads to the desired vaporisation enthalpy of 8H-benzofuran, as shown in Figure 4. The value $\Delta_l^g H_m^o$(298.15 K) = 48.4 ± 1.5 kJ·mol^{-1} [Table 3], estimated in this way is consistent with other results collected for this molecule in Table 3.

The values derived by *CP* and *GA* are summarised in Table 3. For all substances, the enthalpies of vaporisation $\Delta_l^g H_m^o$(298.15 K) evaluated in this way agree well with values obtained from other methods. To obtain more reliable data, the weighted average values

were derived for all species considered in this work (see Table 3). These data were used to calculate the enthalpies of formation for the liquid phase in Section 3.

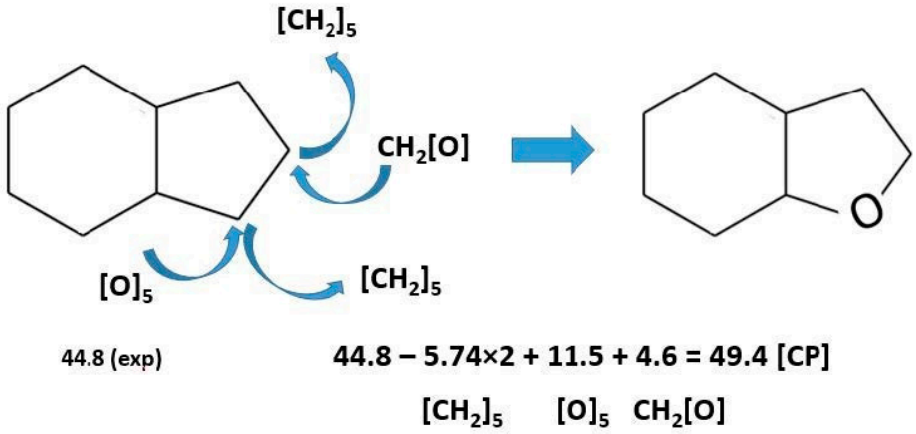

Figure 4. Calculating the enthalpy of vaporisation, $\Delta_l^g H_m^o$(298.15 K)/kJ·mol^{-1} of 8H-benzofuran from 8H-indene using the combination of the centrepiece approach" (*CP*) and the *GA* method. The numerical values of enthalpies of vaporisation required for calculations are given in Tables S6 and S7.

3.2.3. Validation of Vaporisation Enthalpies Using Correlation with the Kovats Indices J_x

A further means of validation are Kovats retention indices, J_x. These can be measured by gas chromatography (GC) [30]. These values represent the strength of interaction between a molecule travelling in the gas phase and the stationary phase during gas chromatography. They can be directly linked to the enthalpy of evaporation. Typically, the $\Delta_l^g H_m^o$(298.15 K) values within a structurally related series of compounds show a linear correlation with Kovats indices [31]. Literature values for furan derivatives on the non-polar column DB-5 (refer to Table 4) were obtained from published studies [32].

Table 4. Correlation of vaporisation enthalpies, $\Delta_l^g H_m^o$(298.15 K)/kJ.mol^{-1} of furan derivatives with their Kovats indices (J_x).

CAS	Compound	J_x [a]	$\Delta_l^g H_m^o$(298.15 K)$_{exp}$ [b]	$\Delta_l^g H_m^o$(298.15 K)$_{calc}$ [c]	Δ [d]
109-99-9	tetrahydrofuran	611	32.6 ± 0.2 [33]	33.1	−0.5
110-00-9	furan	468	27.7 ± 0.2 [33]	27.8	−0.1
1191-99-7	2,3-dihydrofuran	564	31.3 ± 0.3 [34]	31.3	0.0
1708-29-8	2,5-dihydrofuran	614	32.6 ± 0.2 [33]	33.2	−0.6
534-22-5	2-methyl-furan	603	32.7 ± 0.2 [33]	32.7	0.0
625-86-5	2,5-dimethyl-furan	729	37.7 ± 0.2 [33]	37.4	0.3
3208-16-0	2-ethyl-furan	720	37.1 ± 0.2 [33]	37.1	0.0
271-89-6	2,3-benzofuran	1054	48.8 ± 0.3 [12]	49.4	−0.6
496-16-2	2,3-dihydrobenzofuran	1144	53.2 ± 0.4 [13]	52.7	0.5
496-14-0	phthalan	**1142** [e]	53.7 ± 0.4 [14]	52.6	1.1
4265-25-2	2-methyl-benzofuran	1158	53.3 ± 1.5 [35]	53.2	0.1
132-64-9	dibenzofuran	1537	66.3 ± 0.6 [16]	67.2	−0.9

[a] Kovats indices from Table S10, column 5. [b] Experimental data listed in Table 5. [c] Derived from the equation $\Delta_l^g H_m^o$(298.15 K) = 10.46 + 0.0369 × J_x with R^2 = 0.9981, and an expanded uncertainty of ±1.0 kJ.mol^{-1} at the confidence level 0.95, (k = 2). [d] Represents the difference between column 3 and 4 of this table. [e] Data taken from Table S5.

The $\Delta_l^g H_m^o$(298.15 K) values collected in Table 4 show a clear linear correlation with their corresponding J_x-values:

$$\Delta_l^g H_m^o(298.15\text{K})/\text{kJ·mol}^{-1} = 10.46 + 0.0369 \times J_x \text{ with } R^2 = 0.9981 \quad (8)$$

From Table 4, column 6, it is evident that the differences between the measured values and those computed from Equation (8) typically remain under 1.0 kJ·mol^{-1}. The "empirical" enthalpies of vaporisation derived by applying Equation (8) (see column 5) are labelled J_x values in Table 3. Good agreement is observed when compared to results from other methodologies.

Table 5. Compilation of the standard molar entropies of vaporisation, $\Delta_l^g S_m^o$, and the absolute standard molar entropies, S_m^o(g or liq), of HL and HR compounds. (All values at T = 298.15 K in J·K^{-1}·mol^{-1}).

Compound	$\Delta_l^g S_m^o$ [a]	S_m^o(g) [b]	S_m^o(liq) [c]	S_m^o(liq) [d]
2,3-benzofuran [271-89-6]	111.3 ± 0.1 [11]	328.3	215.6 [36]	217.0
isobenzofuran [270-75-7]	102.4 ± 8.0 [g]	330.7		228.3
2,3-dihydro-benzofuran [496-16-2]	119.2 ± 3.0	344.1	226.4 [36]	224.9
1,3-dihydro-isobenzofuran [496-14-0]	119.2 ± 0.1 [14]	357.5		238.3
dibenzofuran [132-64-9]	128.4 ± 2.0 [16]	384.0	248.5 [e]	255.6
fluorene [86-73-7]	136.7 ± 0.4 [37]	392.0	257.8 [f]	255.3
2-coumaranone [553-86-6]	132.4 ± 3.0	353.8		221.4
3-coumaranone [7169-34-8]	132.2 ± 5.1	355.8		223.6
phthalide [87-41-2]	144.5 ± 0.2	353.6		209.1
furan [110-00-9]	93.4 ± 0.2 [38]	272.7	176.7 [38]	179.3
2,3-dihydro-furan [1191-99-7]	95.8 ± 0.1 [34]	294.7		198.9
tetrahydrofuran [109-99-9]	96.5 ± 0.2 [39]	301.7	203.9 [40]	205.2
8H-benzofuran [13054-97-2]	113.1 ± 2.6	365.5		252.4
8H-isobenzofuran [4743-54-8]	110.7 ± 1.4	364.2		253.5
12H-dibenzofuran [13054-98-3]	135.5 ± 4.6	430.7		295.2
12H-fluorene	136.0 ± 2.7	434.7		298.7
6H-2-coumaranone [6051-03-2]	127.6 ± 5.6	373.9		246.3
6H-3-coumaronone [1206676-08-5]	119.8 ± 2.4	377.9		258.1
6H-phthalide [2611-01-0]	162.5 ± 2.9	374.1		211.6
8H-benzofuran-2-ol [36871-99-5]	152.0 ± 8.0 [g]	385.9		233.9
8H-benzofuran-3-ol [99769-38-7]	151.9 ± 5.5	390.3		238.4
8H-isobenzofuran-1-ol [59901-42-7]	172.0 ± 8.0 [g]	387.8		215.8
1,3-cyclopentadiene [542-92-7]		274.5 [41]	182.7 [40]	
cyclopentene [142-29-0]		289.7 [42]	201.3 [43]	
cyclopentane [287-92-3]		292.9	204.1 [44]	
indene [95-13-6]	115.4 ± 0.6 [13]	335.9	214.2 [45]	220.5
indane [496-11-7]	110.8 ± 0.8 [13]	345.9	234.4 [45]	235.1
trans-8H-indene [3296-50-2]	106.2 ± 0.1	371.6	258.9 [46]	265.4

[a] From the vapour pressure values compiled in Table S4 or from the vapour pressure–temperature dependencies given in the corresponding original literature. [b] Calculated with the G3MP2 method. [c] The experimental data available in the literature. [d] Calculated according to Equation (3) using the entries from columns 2 and 3 of this table. [e] Estimated based on the following experimental data from the literature: S_m^o(liq) = S_m^o(cr) + $\Delta_{cr}^l S_m^o$ = 196.2 [15] + 52.3 [15] = 248.5 J·K^{-1}·mol^{-1}. [f] Estimated based on the following experimental data from the literature: S_m^o(liq) = S_m^o(cr) + $\Delta_{cr}^l S_m^o$ = 207.3 [46] + 50.5 [46] = 257.8 J·K^{-1}·mol^{-1}. [f] The assessed value.

3.2.4. Standard Molar Vaporisation Entropies

The connection between standard molar entropies in liquid and gas phases at 298.15 K is established via the standard molar entropy of vaporisation, $\Delta_l^g S_m^o$ (Equation (3)). In this work, the $\Delta_l^g S_m^o$(298.15 K) values have been derived from the intercept of the temperature dependence of vapour pressures as presented in Table S4. The results for $\Delta_l^g S_m^o$(298.15 K) are shown in Table 5, column 2. The gas-phase absolute entropies were calculated using the G3MP2 method (refer to column 3). The liquid phase entropies, estimated according to Equation (3), are shown in Table 5, column 5.

It is important to note that the absolute entropies in the liquid phase, S_m^o(liq), calculated indirectly according to Equation (3) (see Table 5, column 5) based on quantum chemical calculations (Table 5, column 3) agree well with the experimental S_m^o(liq)-values, which were mostly measured using cryogenic adiabatic calorimetry (Table 5, column 4). This agreement confirms the reliability of the sophisticated quantum chemical methods for S_m^o(g) calculations.

3.3. Step III: Thermodynamic Analysis of the LOHC Systems Based on Aromatic Ethers

3.3.1. Reaction Enthalpies, Entropies, and Gibbs Energies of the LOHC Hydrogenation

Hess's Law was used to derive the standard molar enthalpies of chemical reactions, $\Delta_r H_m^o$, from the standard molar enthalpies of formation, $\Delta_f H_m^o$, of the reactants:

$$\Delta_r H_m^o(T) \;=\; \Sigma\Big[\Delta_f H_m^o\,(T,\ \text{products})\Big] \;-\; \Sigma\Big[\ \Delta_f H_m^o(T,\ \text{educts})\Big] \tag{9}$$

Since the $\Delta_f H_m^o$-values for cyclic aliphatic molecules of the hydrogen-rich LOHC counterparts are not available in the literature, they were calculated using the G3MP2 method (see Table S1). This method has proven to be reliable for the alkyl-cyclohexane series in our recent work [47]. The gas phase enthalpies of formation of perhydrogenated aromatic ethers were converted into the required liquid phase enthalpies of formation using the vaporisation enthalpies, $\Delta_l^g H_m^o$(298.15 K), evaluated in Table 3. The $\Delta_f H_m^o$(liq, 298.15 K) values, derived according to Equation (2), are given in Table S11 for the HL compounds and in Table S12 for the HR compounds and can now be used as input variables for Hess's Law according to Equation (9).

The liquid phase reaction enthalpies, $\Delta_r H_m^o$(liq), of the full hydrogenation of aromatic ethers are given in Table S13 and the liquid phase reaction enthalpies, $\Delta_r H_m^o$(liq), of the partial hydrogenation of aromatic ethers are given in Table S14.

The reaction entropies of the hydrogenation of aromatic ethers were calculated according to Equation (10), using the standard molar entropies of the reactants from Table 5 as follows:

$$\Delta_r S_m^o(T) \;=\; \Sigma[S_m^o\,(T,\ \text{products})] \;-\; \Sigma[S_m^o(T,\ \text{educts})] \tag{10}$$

The resulting total liquid phase reaction entropies, $\Delta_r S_m^o$(liq, 298.15 K), of the hydrogenation reactions with LOHC candidates are shown in Figure 2, as compiled in Table S15.

The Gibbs energies for the liquid phase for the hydrogenation reactions are reported in Table S15. The calculations have initially been carried out at the reference temperature T = 298 K. Utilising the standard molar isobaric heat capacities $C_{p,m}^o$ of the reactants, the reaction's thermodynamic feasibility can be evaluated at any temperature through Kirchhoff's law and the van't-Hoff equation. The change in reaction enthalpies and entropies as a function of temperature is determined by these thermodynamic relations

$$\Delta_r H_m^o(\text{liq}, T) = \Delta_r H_m^o(\text{liq}, 298.15\ \text{K}) + \Delta_r C_{p,m}^o(\text{liq}) \times \Big(T - 298.15\ \text{K}\Big) \tag{11}$$

$$\Delta_r S_m^o(\text{liq}, T) = \Delta_r S_m^o(\text{liq}, 298.15\ \text{K}) + \Delta_r C_{p,m}^o(\text{liq}) \times \ln(T/298.15\ \text{K}) \tag{12}$$

where $\Delta_r C^o_{p,m}(\mathrm{liq})$ denotes the change in heat capacity throughout the reaction. This value is computed following Hess's Law principles, based on standard molar heat capacities, $C^o_{p,m}(\mathrm{liq})$, of reaction participants with the stoichiometric coefficients as weighting factors (see Table S5). These values depend on temperature and are not available for all potential LOHC structures (this particularly holds for the hydrogenated forms). Nevertheless, even though the $C^o_{p,m}(\mathrm{liq})$ values for the individual species might be large, the $\Delta_r C^o_{p,\,m}$ values for reactions are generally quite small and change little over temperature as the effects of reactants and products cancel each other. Therefore, in this work the $\Delta_r C^o_{p,\,m}$ values at 298.15 K have been utilised for the adjustment of $\Delta_r H^o_m(\mathrm{liq}, T)$ and $\Delta_r S^o_m(\mathrm{liq}, T)$ to T = 500 K, as well as for the calculation of $\Delta_r G^o_m(500\ \mathrm{K})$ values, which are shown in Table S15. Uncertainties for $\Delta_r G^o_m(500\ \mathrm{K})$ values are not provided due to the lack of validated experimental benchmark data at this temperature. While such uncertainties can be estimated at 298 K using reference data for standard enthalpies of formation, no comparable data set exists for 500 K. In particular, reliable entropy data from adiabatic calorimetry are scarce.

3.3.2. Comparison of the Thermodynamics of Hydrogenation Reactions with and Without Oxygen Functionality

Detailed information on the calculations leading to the thermodynamic parameters of the hydrogenation/dehydrogenation reactions is provided in the electronic supplementary information (Tables S9–S13). The final results for the enthalpies of the liquid phase reaction enthalpies, $\Delta_r H^o_m$, reaction entropies, $\Delta_r S^o_m$, Gibbs energies, $\Delta_r G^o_m$, and equilibrium temperatures, T_{eq}, are summarised in Table 6 for discussion and comparison.

Table 6. The liquid phase reaction enthalpies, $\Delta_r H^o_m$, reaction entropies, $\Delta_r S^o_m$, Gibbs energies, $\Delta_r G^o_m$, and equilibrium temperatures, T_{eq}, of the full hydrogenation reactions of aromatic ethers given in Figure 2, (p° = 0.1 MPa).

Compound	$\Delta_r H^o_m$(298 K)/H_2 [d]	$\Delta_r S^o_m$(298 K)/H_2	$\Delta_r G^o_m$(298 K)/H_2 [b]	$\Delta_r G^o_m$(500 K)/H_2 [b]	$\Delta_r H^o_m$(298 K)	$\Delta_r S^o_m$(298 K)	$\Delta_r G^o_m$(298 K) [b]	$\Delta_r G^o_m$(500 K) [b]	T_{eq}
	kJ·mol^{-1}	J·K^{-1}·mol^{-1}	kJ·mol^{-1}	kJ·mol^{-1}	kJ·mol^{-1}	J·K^{-1}·mol^{-1}	kJ·mol^{-1}	kJ·mol^{-1}	K
(aliphatic)$_5$									
1,3-cyclopentadiene	**−105.5**	−120.0	−69.7	−44.2	−211.0	−240.0	−139.4	−88.4	**879**
furan	−77.0	−117.1	−42.0	−17.0	−153.9	−234.2	−84.1	−34.0	697
(aromatic)$_6$ + *(aliphatic)*$_5$									
indene	**−71.7**	−119.5	−72.1	−10.6	−286.8	−478.1	−144.3	−42.5	**600**
2,3-benzofuran	−62.1	−121.5	−25.8	−0.1	−248.2	−486.0	−103.3	−0.5	511
2,3-dihydrobenzofuran	−61.1	−122.0	−24.7	1.2	−183.2	−366.1	−74.0	3.5	500
isobenzofuran	−76.1	−124.4	−39.0	−16.0	−304.3	−497.6	−155.9	−63.9	612
1,3-dihydro-isobenzofuran	−63.3	−125.6	−25.9	−2.6	−190.0	−376.9	−77.6	−7.7	504
(aromatic)$_6$ + *(aliphatic)*$_5$ +*(aromatic)*$_6$									
fluorene	**−59.0**	−123.9	−22.1	4.1	−354.2	−743.3	−132.6	24.6	**477**
dibenzofuran	−57.3	−124.1	−20.3	6.1	−343.7	−744.6	−121.7	36.6	462
(aromatic)$_6$ + *(lactone)*$_5$									
indene	**−71.7**	−119.5	−72.1	−10.6	−286.8	−478.1	−144.3	−42.5	**600**
2-coumaranone	−55.1	−127.6	−17.0	9.7	−220.2	−510.3	−68.1	38.9	432
3-coumaranone	−59.9	−127.0	−22.0	4.9	−239.4	−508.0	−87.9	19.5	471
phthalide	−48.7	−129.0	−10.3	16.8	−194.9	−516.1	−41.0	67.1	378
open-chained ethers									
benzene	**−68.5**	−120.3	−32.6	−7.0	−205.4	−360.9	−97.8	−21.1	**569**
methoxy-benzene	−65.6	−118.9	−30.1	−4.6	−196.8	−356.8	−90.4	−13.7	552
diphenyl ether	−68.1	−126.2	−30.5	−3.8	−408.5	−757.3	−182.7	−22.6	539

[a] Liquid-phase formation enthalpies of hydrocarbons and aromatic ethers (HL counterparts from Table S11). [b] Liquid-phase enthalpies of formation of hydrocarbons and perhydrogenated aromatic ethers (HR counterparts from Table S12). [c] Values calculated using Hess's Law applied to the aromatic ether reactions shown in Figure 2. [d] Reaction enthalpy per mole H_2.

As a preliminary assessment, the thermodynamic suitability of a compound as a hydrogen storage material is often evaluated based on the reaction enthalpies of hydrogenation at 298.15 K. The relevant benchmark in this context is approximately –63 kJ·mol^{-1}, which is characteristic of commercial hydrogen storage materials. However, from a thermodynamic perspective, the key parameter is the Gibbs reaction energy. This value should be as large as possible to enable hydrogen release at temperatures below 500 K. The data relevant for comparing the suitability of the different compounds as hydrogen storage materials are shown in Table 6.

3.3.3. Comparison of Reactions Involving Five-Membered Aliphatic Rings

First of all, it is interesting to compare the thermodynamic characteristics of the hydrogenation reactions for 1,3-cyclopentadiene and furan (see Figure 5).

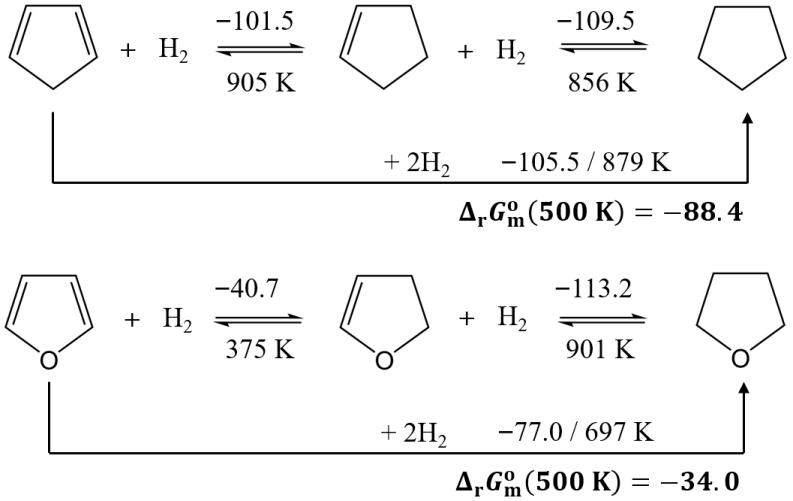

Figure 5. Comparison of the thermodynamic characteristics of the hydrogenation reactions for 1,3-cyclopentadiene and furan. The numerical values for reaction enthalpies, $\Delta_r H_m^o$(298 K), are given above the arrows (in kJ·mol^{-1}/H$_2$) and the T_{eq} values are given below the arrows in K. Gibbs reaction energies of full hydrogenation, $\Delta_r G_m^o$(500 K) are given in kJ·mol^{-1}.

In this system, there is a substantial difference in the hydrogenation reaction enthalpies of nearly 30 kJ·mol^{-1}/H$_2$. In both cases, the full hydrogenation reactions remain strongly exergonic even at 500 K (−88.4 kJ·mol^{-1} for 1,3-cyclopentadiene and −34.0 kJ·mol^{-1} for furan). As a result, these compounds enable stable hydrogen storage in terms of neglectable dehydrogenation; however, the energy required for hydrogen release would be unacceptably high. It is noteworthy that the hydrogenation steps in 1,3-cyclopentadiene exhibit approximately the same reaction enthalpy, whereas a pronounced difference is observed in the case of furan. Interestingly, the first hydrogenation step of furan is associated with a remarkably low reaction enthalpy of −40.7 kJ·mol^{-1}/H$_2$. The selective and reversible hydrogenation of a single double bond could therefore represent a largely unexplored approach to hydrogen storage.

3.3.4. Comparison of Reactions Involving Aromatic Ethers with Attached Five-Membered Aliphatic Ring

The condensation of an aromatic ring onto the 1,3-cyclopentadiene or furan backbone significantly alters the enthalpy difference for hydrogenation (see Figure 6). The difference in reaction enthalpies of the full hydrogenation is reduced to approximately 10 kJ·mol^{-1}/H$_2$ between benzofuran and indene. Moreover, the hydrogenation enthalpies of the benzofuran systems decrease to roughly −62 kJ·mol^{-1}/H$_2$, which is comparable to the typical values

observed for commercial hydrogen carriers. Partial hydrogenation is not advantageous for these compounds. In indene, benzofuran, and isobenzofuran, the hydrogenation of the first double bond is significantly more exothermic than subsequent steps. According to the Gibbs free energy of reaction, dehydrogenation becomes thermodynamically favourable for 8H-benzofuran at temperatures above approximately 500 K. Thermodynamically, this represents a significant advantage for its application as a hydrogen storage material.

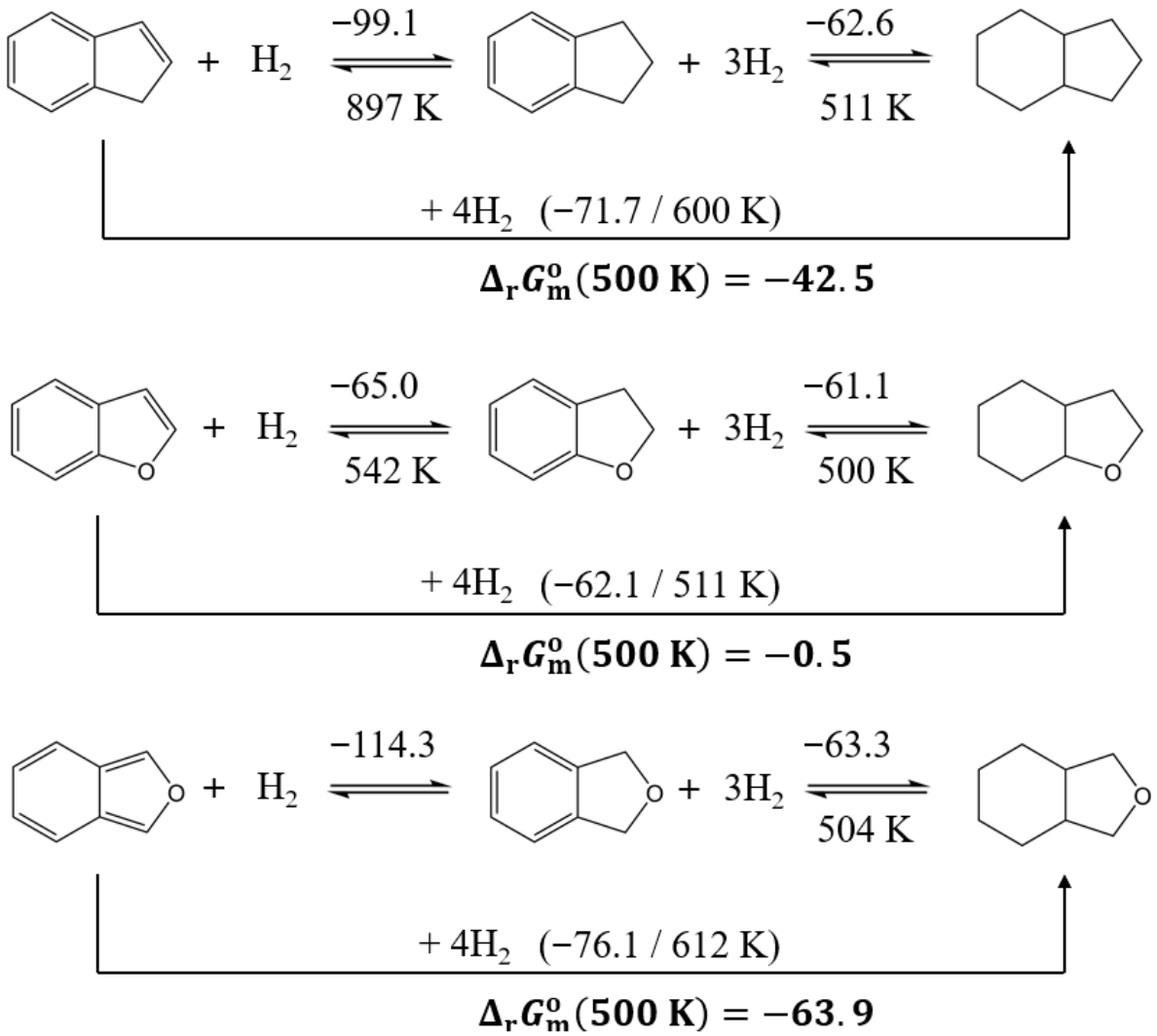

Figure 6. Comparison of the thermodynamic characteristics of the hydrogenation reactions for benzofuran derivatives. The numerical values for reaction enthalpies, $\Delta_r H_m^o$(298 K), are given above the arrows (in kJ·mol^{-1}/H$_2$) and the T_{eq} values are given below the arrows in K. Gibbs reaction energies of full hydrogenation, $\Delta_r G_m^o$(500 K), are given in kJ·mol^{-1}.

3.3.5. Comparison of Reactions Involving a Five-Membered Aliphatic Ring Fused to Two Benzene Rings

There is no longer a significant difference in the reaction enthalpies of fluorene and dibenzofuran hydrogenation, with both values ranging between approximately (−57 to −59) kJ·mol^{-1}/H$_2$. The condensation of an additional aromatic ring further reduces the enthalpy gap between the pure hydrocarbon and the furan derivative, as already seen in the benzofuran systems. Furthermore, the Gibbs free reaction energies for hydrogenation at 500 K are strongly positive, with values of −24.6 kJ·mol^{-1} for fluorene and −36.6 kJ·mol^{-1} for dibenzofuran (see Figure 7). This indicates that high hydrogen yields during dehydrogenation can already be expected at temperatures below 500 K.

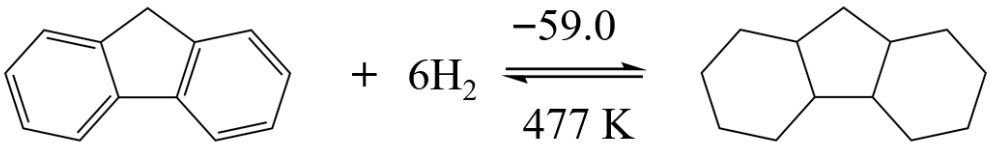

$$\Delta_r G^o_m(500\ \mathrm{K}) = 26.3$$

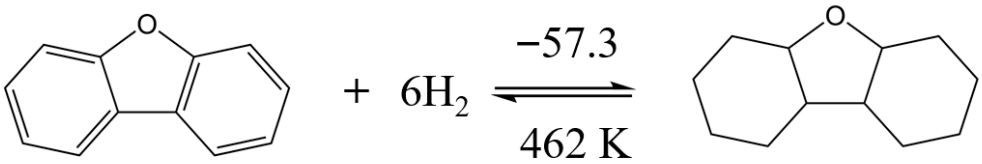

$$\Delta_r G^o_m(500\ \mathrm{K}) = 36.6$$

Figure 7. Comparison of the thermodynamic characteristics of the hydrogenation reactions for fluorene and dibenzofuran. The numerical values for reaction enthalpies, $\Delta_r H^o_m$(298 K), are given above the arrows (in kJ·mol^{-1}/H_2) and the T_{eq} values are given below the arrows in K. Gibbs reaction energies of full hydrogenation, $\Delta_r G^o_m$(500 K), are given in kJ·mol^{-1}.

3.3.6. Could the Lactone Ring Improve Hydrogen Storage Thermodynamics?

In comparison to benzofurans, lactones exhibit a lower reaction enthalpy for the full hydrogenation because of the possible hydrogenation of the keto group to a hydroxy group. Regarding the hydrogenation of the aromatic ring, the reaction enthalpy for 2-coumaranone (−67.5 kJ·mol^{-1}/H_2) and phthalide (−64.4 kJ·mol^{-1}/H_2) is not favourable in comparison to commercial LOHCs (see Figure 8). Moreover, the absolute values of the hydrogenation enthalpies of the keto group are so low that long-term hydrogen storage is not feasible.

The most promising candidate among the lactones is 3-coumaranone with a complete hydrogenation reaction enthalpy −59.9 kJ·mol^{-1}/H_2 and possible dehydrogenation below 500 K. In addition, the hydrogenation enthalpies of the aromatic ring (−57.1 kJ·mol^{-1}) and the keto group (−68.1 kJ·mol^{-1}) are of a similar magnitude (see Figure 8).

3.3.7. Thermodynamic Analysis of the Reversible Hydrogenation/Dehydrogenation Process

Generally, hydrogen release from the hydrogen-rich form of a LOHC is thermodynamically more challenging than the hydrogen charging reaction [48]. Suitability as a hydrogen storage material is assessed based on the magnitude of the Gibbs reaction energy at 500 K, with higher values indicating greater potential. When comparing the Gibbs reaction enthalpies in Table 6, it is important to consider the differing values associated with the various degrees of hydrogenation. For lactones, in particular, a significant difference is observed between the hydrogenation of the aromatic ring and that of the hydroxyl group. Although 2-coumaranone, 3-coumaranone, and phthalide exhibit very high values, these are primarily due to the hydrogenation of the keto group. Hydrogenation of the aromatic ring is more favourable than in established hydrogen carriers only in the case of 3-coumaranone.

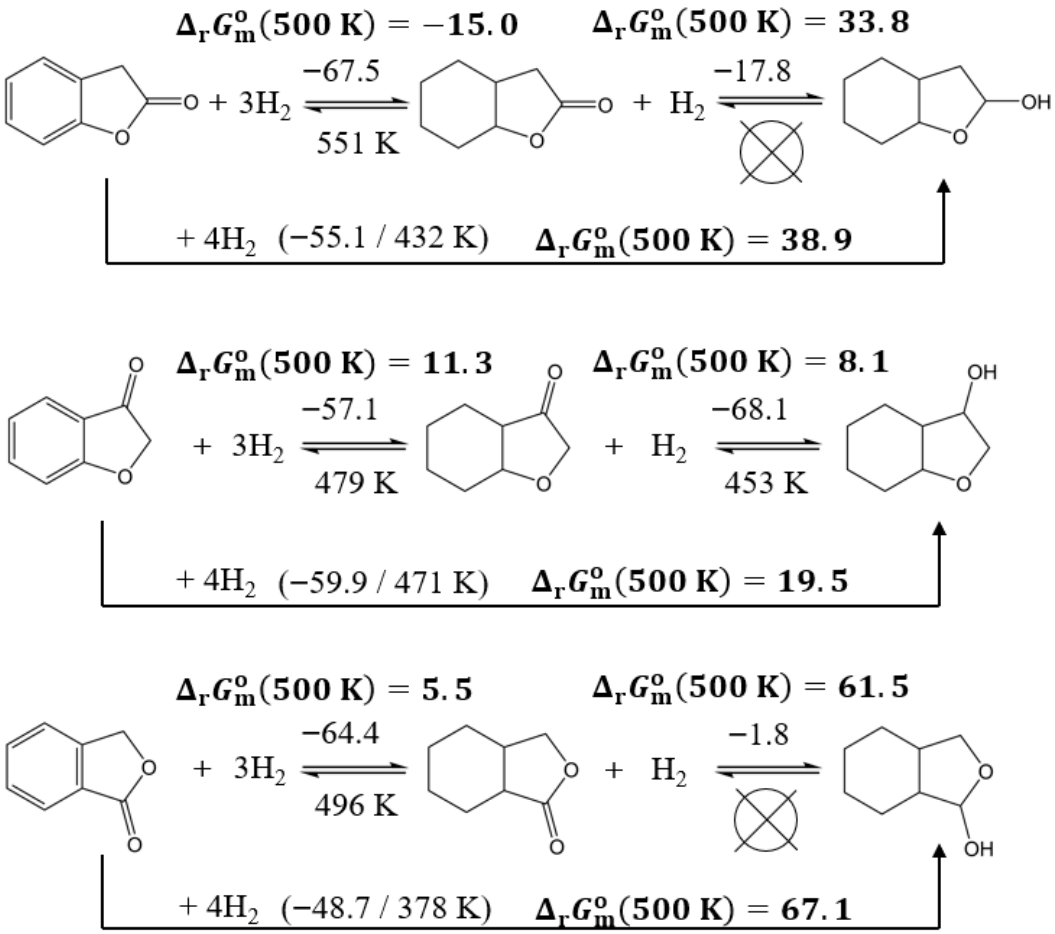

Figure 8. Comparison of the thermodynamic characteristics of the hydrogenation reactions for aromatic lactones. The numerical values for reaction enthalpies, $\Delta_r H_m^o$(298 K), are given above the arrows (in kJ·mol^{-1}/H_2) and the T_{eq}-values are given below the arrows in K. Gibbs reaction energies of full hydrogenation, $\Delta_r G_m^o$(500 K) are given in kJ·mol^{-1}.

The addition of aromatic rings to the furan backbone leads to increasingly favourable properties for dehydrogenation. The benzofuran derivatives containing one aromatic ring already exhibit Gibbs reaction enthalpies comparable to those of typical hydrogen carriers. The condensation of an additional ring further amplifies this effect. Alternatively, a lactone may form in place of the second ring. However, dibenzofuran possesses the most favourable Gibbs reaction energy of the compounds investigated in this work. For this reason, lactone formation is comparatively less advantageous in comparison to the addition of the second aromatic ring.

4. Conclusions

This study demonstrates that the incorporation of oxygen functionalities into bi- and tricyclic aromatic compounds containing five-membered rings significantly influences their thermodynamic properties as liquid organic hydrogen carriers (LOHCs). The combined use of experimental vaporisation data and high-level quantum chemical calculations allowed for the reliable estimation of reaction enthalpies and entropies, confirming that the optimal balances of these parameters could enable effective hydrogen release at moderate temperatures below 500 K. Thermodynamic evaluation based on Gibbs reaction energies at 500 K reveals that dibenzofuran exhibits the most favourable characteristics, with a Gibbs energy of 36.6 kJ·mol^{-1}, indicating high potential for efficient hydrogen storage and release. In contrast, lactone formation offers comparatively less advantage for hydrogen

storage applications. In summary, aromatic furan derivatives with extended ring systems, particularly low melting dibenzofuran derivatives, emerge as promising candidates for LOHC materials.

Supplementary Materials: The following supporting information can be downloaded at: https://www.mdpi.com/article/10.3390/oxygen5030018/s1, Table S1: Results of quantum-chemical calculations with G3MP2 method for aromatic ethers and lactones and their hydrogenated products; Table S2: Results of quantum-chemical calculations with G3MP2/B3LYP method by Notario et al. for aromatic ethers; Table S3: Enthalpies of fusion vaporization and sublimation of aromatic ethers and auxiliary compounds at melting points and 298 K; Table S4: The vapour pressures and standard vaporisation enthalpies and entropies obtained by the approximation of boiling points at different pressures available in the literature; Table S5: Compilation of data on molar heat capacities heat capacity differences at T = 298.15 K; Table S6: Thermochemical data at for reference compounds; Table S7: Compilation of the standard molar enthalpies of vaporization for auxiliary compounds; Table S8: Correlation of vaporisation enthalpies, of auxiliary compounds with their Kovats indices; Table S9: Group-additivity values for calculation of enthalpies of vaporization of alkanes, ethers, ketones, alcohols and esters at 298.15 K; Table S10: Correlation of the normal boiling temperatures of furan derivatives with their Kovats retention indices; Table S11: Calculation of the liquid-phase enthalpies of formation for the hydrogen lean compounds; Table S12: Calculation of the liquid-phase enthalpies of formation for the hydrogen rich compounds; Table S13: Calculation of the liquid phase reaction enthalpies of the full hydrogenation reactions of aromatic; Table S14: Calculation of the liquid phase reaction enthalpies of the partial hydrogenation of aromatic compounds; Table S15. Liquid phase thermodynamic properties of the hydrogenation of the hydrogen-lean LOHC counterparts; Table S16: Comparison of the hydrogen storage capacity values of LOHC candidates in different common units. Figure S1. Structures of the most stable conformers of aromatic ethers, lactones and their hydrogenated products. Figure S2. Well balanced reaction used in ref. [10] for calculations of standard molar enthalpies of formation, $\Delta_f H^o_m(g)$, from the G3MP2 and G3MP2/B3LYP methods. Figure S3. Calculating the enthalpy of vaporization, $\Delta^g_l H^o_m(298.15\ K)/kJ\ mol^{-1}$ of 8H-benzofuran using the "centerpiece approach" (CP) and using the GA method. The numerical values of enthalpies of vaporisation required for calculations are given in Table S6 and the group-contributions are given in Table S7. Figure S4. Calculating the enthalpy of vaporization, $\Delta^g_l H^o_m(298.15\ K)/kJ\ mol^{-1}$ of 8H-isobenzofuran using the "centerpiece approach" (CP) and using the GA method. The numerical values of enthalpies of vaporisation required for calculations are given in Table S6 and the group-contributions are given in Table S7. Figure S5. Calculating the enthalpy of vaporization, $\Delta^g_l H^o_m(298.15\ K)/kJ\ mol^{-1}$ of 2-coumaranone using the "centerpiece approach" (CP) and 2,3-dihydrobenzofuran or 2-indanone as the staring molecules. The numerical values of enthalpies of vaporisation required for calculations are given in Tables 3 and S6. Figure S6. Calculating the enthalpy of vaporization, $\Delta^g_l H^o_m(298.15\ K)/kJ\ mol^{-1}$ of 3-coumaranone using the "centerpiece approach" (CP) and indane, 2,3-dihydrobenzofuran or 2-indanone as the staring molecules. The numerical values of enthalpies of vaporisation required for calculations are given in Tables 3 and S6. Figure S7. Calculating the enthalpy of vaporization, $\Delta^g_l H^o_m(298.15\ K)/kJ\ mol^{-1}$ of phthalide using the "centerpiece approach" (CP) and indane, phthalan or 1-indanone as the staring molecules. The numerical values of enthalpies of vaporisation required for calculations are given in Tables 3 and S6. Figure S8. Calculating the enthalpy of vaporization, $\Delta^g_l H^o_m(298.15\ K)/kJ\ mol^{-1}$ of 6H-phthalide using the "centerpiece approach" (CP) and 8H-indene, 8H-benzofuran or 6H-1-indanone as the staring molecules. The numerical values of enthalpies of vaporisation required for calculations are given in Tables 3 and S6. Figure S9. Calculating the enthalpy of vaporization, $\Delta^g_l H^o_m(298.15\ K)/kJ\ mol^{-1}$ of 6H-2-coumaranone, 3-coumaranon, and 6H-phthalide using the "centerpiece approach" (CP) and 2-coumaranone, 3-coumaranone, and phthalide as the staring molecules. The numerical values of enthalpies of vaporisation required for calculations are given in Tables 3 and S6. Figure S10. Calculating the enthalpy of vaporization, $\Delta^g_l H^o_m(298.15\ K)/kJ\ mol^{-1}$ of 8H-benzofuran-2-ol, 8H-benzofuran-3-ol, and 8H-benzofuran-1-ol using the "centerpiece approach"

(CP) and 8H-indene, 8H-benzofuran or 8H-isobenzofuran as the staring molecules. The numerical values of enthalpies of vaporisation required for calculations are given in Tables 3 and S6.

Author Contributions: Conceptualization, R.S., S.P.V., K.M. and P.W.; methodology, R.S. and S.P.V.; software, A.A.S.; validation, R.S., S.V.V. and S.P.V.; formal analysis, R.S. and S.V.V.; investigation, R.S. and S.V.V.; resources, K.M.; data curation, R.S., S.V.V. and S.P.V.; writing—original draft preparation, R.S. and S.P.V.; writing—review and editing, S.V.V., A.A.S., K.M. and P.W.; visualisation, A.A.S.; supervision, S.P.V.; project administration, S.P.V. and K.M.; funding acquisition, K.M. and P.W. All authors have read and agreed to the published version of the manuscript.

Funding: This project has been funded by the Free State of Bavaria through the project "Oxo-LOHC-Autotherme und ultratiefe Wasserstoff-Freisetzung aus LOHC-Systeme-Oxo-LOHC" (grant number: 84-6665a2/201/11).

Data Availability Statement: All data are available in the text and in the electronic supporting information.

Acknowledgments: AAS gratefully acknowledges the Committee on Science and Higher Education of the Government of St. Petersburg. This work was partly supported by the Ministry of Science and Higher Education of the Russian Federation (theme No. FSSE-2025-0006) as part of the state task of the Samara State Technical University (creation of new youth laboratories).

Conflicts of Interest: The authors declare no conflicts of interest.

References

1. Teichmann, D.; Arlt, W.; Wasserscheid, P.; Freymann, R. A Future Energy Supply Based on Liquid Organic Hydrogen Carriers (LOHC). *Energy Environ. Sci.* **2011**, *4*, 2767. [CrossRef]
2. Zakgeym, D.; Hofmann, J.D.; Maurer, L.A.; Auer, F.; Müller, K.; Wolf, M.; Wasserscheid, P. Better through Oxygen Functionality? The Benzophenone/Dicyclohexylmethanol LOHC-System. *Sustain. Energy Fuels* **2023**, *7*, 1213–1222. [CrossRef]
3. Verevkin, S.P.; Samarov, A.A.; Vostrikov, S.V. Does the Oxygen Functionality Really Improve the Thermodynamics of Reversible Hydrogen Storage with Liquid Organic Hydrogen Carriers? *Oxygen* **2024**, *4*, 266–284. [CrossRef]
4. Ghahremanpour, M.M.; van Maaren, P.J.; Ditz, J.C.; Lindh, R.; van der Spoel, D. Large-Scale Calculations of Gas Phase Thermochemistry: Enthalpy of Formation, Standard Entropy, and Heat Capacity. *J. Chem. Phys.* **2016**, *145*, 114305. [CrossRef]
5. Pracht, P.; Bohle, F.; Grimme, S. Automated Exploration of the Low-Energy Chemical Space with Fast Quantum Chemical Methods. *Phys. Chem. Chem. Phys.* **2020**, *22*, 7169–7192. [CrossRef]
6. Frisch, M.J.; Trucks, G.W.; Schlegel, H.B.; Scuseria, G.E.; Robb, M.A.; Cheeseman, J.R.; Scalmani, G.; Barone, V.; Petersson, G.A.; Nakatsuji, H.; et al. *Gaussian 16, Revision C.01*; Gaussian, Inc.: Wallingford, CT, USA, 2016.
7. Wheeler, S.E.; Houk, K.N.; Schleyer, P.v.R.; Allen, W.D. A Hierarchy of Homodesmotic Reactions for Thermochemistry. *J. Am. Chem. Soc.* **2009**, *131*, 2547–2560. [CrossRef] [PubMed]
8. Verevkin, S.P.; Emel'yanenko, V.N.; Notario, R.; Roux, M.V.; Chickos, J.S.; Liebman, J.F. Rediscovering the Wheel. Thermochemical Analysis of Energetics of the Aromatic Diazines. *J. Phys. Chem. Lett.* **2012**, *3*, 3454–3459. [CrossRef] [PubMed]
9. Notario, R.; Victoria Roux, M.; Castaño, O. The Enthalpy of Formation of Dibenzofuran and Some Related Oxygen-Containing Heterocycles in the Gas Phase. A GAUSSIAN-3 Theoretical Study. *Phys. Chem. Chem. Phys.* **2001**, *3*, 3717–3721. [CrossRef]
10. Sousa, C.C.S.; Matos, M.A.R.; Santos, L.M.N.B.F.; Morais, V.M.F. Reprint of: Energetics of 2- and 3-Coumaranone Isomers: A Combined Calorimetric and Computational Study. *J. Chem. Thermodyn.* **2014**, *73*, 283–289. [CrossRef]
11. Steele, W.V.; Chirico, R.D. *Cooperative Agreement No. FC22-83FE60149 (NIPEP-457)*; IIT Research Institute, NIPEP: Bartlesville, OK USA, 1990; pp. 1–75.
12. Verevkin, S.P.; Emel'yanenko, V.N.; Pimerzin, A.A.; Vishnevskaya, E.E. Thermodynamic Analysis of Strain in Heteroatom Derivatives of Indene. *J. Phys. Chem. A* **2011**, *115*, 12271–12279. [CrossRef]
13. Verevkin, S.P.; Emel'yanenko, V.N.; Pimerzin, A.A.; Vishnevskaya, E.E. Thermodynamic Analysis of Strain in the Five-Membered Oxygen and Nitrogen Heterocyclic Compounds. *J. Phys. Chem. A* **2011**, *115*, 1992–2004. [CrossRef]
14. Steele, W.V.; Chirico, R.D.; Knipmeyer, S.E.; Nguyen, A.; Smith, N.K.; Tasker, I.R. Thermodynamic Properties and Ideal-Gas Enthalpies of Formation for Cyclohexene, Phthalan (2,5-Dihydrobenzo-3,4-Furan), Isoxazole, Octylamine, Dioctylamine, Trioctylamine, Phenyl Isocyanate, and 1,4,5,6-Tetrahydropyrimidine. *J. Chem. Eng. Data* **1996**, *41*, 1269–1284. [CrossRef]
15. Chirico, R.; Gammon, B.; Knipmeyer, S.; Nguyen, A.; Strube, M.; Tsonopoulos, C.; Steele, W. The Thermodynamic Properties of Dibenzofuran. *J. Chem. Thermodyn.* **1990**, *22*, 1075–1096. [CrossRef]
16. Verevkin, S.P. Enthalpy of Sublimation of Dibenzofuran: A Redetermination. *Phys. Chem. Chem. Phys.* **2003**, *5*, 710–712. [CrossRef]

17. Rakus, K.; Verevkin, S.P.; Schätzer, J.; Beckhaus, H.; Rüchardt, C. Thermolabile Hydrocarbons, 33. Thermochemistry and Thermal Decomposition of 9,9′-Bifluorenyl and 9,9′-Dimethyl-9,9′-bifluorenyl—The Stabilization Energy of 9-Fluorenyl Radicals. *Chem. Ber.* **1994**, *127*, 1095–1103. [CrossRef]
18. Verevkin, S.P. Vapor Pressure Measurements on Fluorene and Methyl-Fluorenes. *Fluid Phase Equilib.* **2004**, *225*, 145–152. [CrossRef]
19. Tavernier, P. Donnees Thermochimiques Relatives Aux Constituants Des Poudres. *Mem. Poudres* **1956**, 301–327.
20. Freitas, V.L.S.; Santos, C.P.F.; Ribeiro da Silva, M.D.M.C.; Ribeiro da Silva, M.A.V. The Effect of Ketone Groups on the Energetic Properties of Phthalan Derivatives. *J. Chem. Thermodyn.* **2016**, *96*, 74–81. [CrossRef]
21. Stephenson, R.M.; Malanowski, S. *Handbook of the Thermodynamics of Organic Compounds*; Springer: Dordrecht, The Netherlands, 1987; ISBN 978-94-010-7923-5.
22. Gobble, C.; Chickos, J.S. The Vapor Pressure and Vaporization Enthalpy of R-(+)-Menthofuran, a Hepatotoxin Metabolically Derived from the Abortifacient Terpene, (R)-(+)-Pulegone by Correlation Gas Chromatography. *J. Chem. Thermodyn.* **2016**, *98*, 135–139. [CrossRef]
23. Stull, D.R. Vapor Pressure of Pure Substances. Organic and Inorganic Compounds. *Ind. Eng. Chem.* **1947**, *39*, 517–540. [CrossRef]
24. Verevkin, S.P. Weaving a Web of Reliable Thermochemistry around Lignin Building Blocks: Phenol, Benzaldehyde, and Anisole. *J. Therm. Anal. Calorim.* **2022**, *147*, 6073–6085. [CrossRef]
25. Verevkin, S.P.; Samarov, A.A.; Vostrikov, S.V. Thermodynamics of Reversible Hydrogen Storage: Are Methoxy-Substituted Biphenyls Better through Oxygen Functionality? *Hydrogen* **2023**, *4*, 862–880. [CrossRef]
26. Samarov, A.A.; Verevkin, S.P. Hydrogen Storage Technologies: Methyl-Substituted Biphenyls as an Auspicious Alternative to Conventional Liquid Organic Hydrogen Carriers (LOHC). *J. Chem. Thermodyn.* **2022**, *165*, 106648. [CrossRef]
27. Verevkin, S.P.; Andreeva, I.V.; Zherikova, K.V.; Pimerzin, A.A. Prediction of Thermodynamic Properties: Centerpiece Approach—How Do We Avoid Confusion and Get Reliable Results? *J. Therm. Anal. Calorim.* **2022**, *147*, 8525–8534. [CrossRef]
28. Benson, S.W. *Thermochemical Kinetics*, 2nd ed.; John Wiley & Sons: New York, NY, USA; London, UK; Sydney, Australia; Toronto, ON, Canada, 1976; pp. 1–320.
29. Verevkin, S.P.; Emel'yanenko, V.N.; Diky, V.; Muzny, C.D.; Chirico, R.D.; Frenkel, M. New Group-Contribution Approach to Thermochemical Properties of Organic Compounds: Hydrocarbons and Oxygen-Containing Compounds. *J. Phys. Chem. Ref. Data* **2013**, *42*, 033102. [CrossRef]
30. Kováts, E. Gas-chromatographische Charakterisierung Organischer Verbindungen. Teil 1: Retentionsindices Aliphatischer Halogenide, Alkohole, Aldehyde Und Ketone. *Helv. Chim. Acta* **1958**, *41*, 1915–1932. [CrossRef]
31. Verevkin, S.P. Vapour Pressures and Enthalpies of Vaporization of a Series of the Linear N-Alkyl-Benzenes. *J. Chem. Thermodyn.* **2006**, *38*, 1111–1123. [CrossRef]
32. NIST Chemistry WebBook. Available online: https://webbook.nist.gov/chemistry/ (accessed on 15 June 2025).
33. Majer, V.; Svoboda, V. *Enthalpies of Vaporization of Organic Compounds: A Critical Review and Data Compilation*; Blackwell Scientific Publications: Oxford, UK, 1985; pp. 1–300. Available online: http://old.iupac.org/publications/books/author/majer.html (accessed on 15 June 2025).
34. Steele, W.V.; Chirico, R.D.; Knipmeyer, S.E.; Nguyen, A. Measurements of Vapor Pressure, Heat Capacity, and Density along the Saturation Line for Cyclopropane Carboxylic Acid, N, N -Diethylethanolamine, 2,3-Dihydrofuran, 5-Hexen-2-One, Perfluorobutanoic Acid, and 2-Phenylpropionaldehyde. *J. Chem. Eng. Data* **2002**, *47*, 715–724. [CrossRef]
35. Steele, W.V.; Chirico, R.D.; Knipmeyer, S.E.; Nguyen, A.; Tasker, I.R. *Determination of Ideal Gas Enthalpies of Formation for Key Compounds the 1991 Project Results*; DIPPR Project, NIPER-716; National Inst. for Petroleum and Energy Research: Bartlesville, OK, USA, 1993.
36. Chirico, R.D.; Nguyen, A.; Steele, W.V.; Strube, M.M.; Hossenlopp, I.A.; Gammon, B.E. Thermochemical and Thermophysical Properties of Organic Compounds Derived from Fossil Substances. Chemical Thermodynamic Properties of Organic Oxygen Compounds Found in Fossil Materials. *NIPER Rep.* **1986**, *135*, 1–42.
37. Sasse, K.; Jose, J.; Merlin, J.-C. A Static Apparatus for Measurement of Low Vapor Pressures. Experimental Results on High Molecular-Weight Hydrocarbons. *Fluid Phase Equilib.* **1988**, *42*, 287–304. [CrossRef]
38. Guthrie, G.B.; Scott, D.W.; Hubbard, W.N.; Katz, C.; McCullough, J.P.; Gross, M.E.; Williamson, K.D.; Waddington, G. Thermodynamic Properties of Furan. *J. Am. Chem. Soc.* **1952**, *74*, 4662–4669. [CrossRef]
39. Parsana, V.M.; Parikh, S.; Ziniya, K.; Dave, H.; Gadhiya, P.; Joshi, K.; Gandhi, D.; Vlugt, T.J.H.; Ramdin, M. Isobaric Vapor–Liquid Equilibrium Data for Tetrahydrofuran + Acetic Acid and Tetrahydrofuran + Trichloroethylene Mixtures. *J. Chem. Eng. Data* **2023**, *68*, 349–357. [CrossRef]
40. Lebedev, B.V.; Lityagov, V.Y. Calorimetric Study of Tetrahydrofuran and Its Polymerization in the Temperature Range 0–400 °K. *Vysok. Soedin.* **1977**, *A19*, 2283–2290. [CrossRef]
41. Furuyama, S.; Golden, D.M.; Benson, S.W. Thermochemistry of Cyclopentene and Cyclopentadiene from Studies of Gas-Phase Equilibria. *J. Chem. Thermodyn.* **1970**, *2*, 161–169. [CrossRef]

42. Beckett, C.W.; Freeman, N.K.; Pitzer, K.S. The Thermodynamic Properties and Molecular Structure of Cyclopentene and Cyclohexene 1. *J. Am. Chem. Soc.* **1948**, *70*, 4227–4230. [CrossRef]
43. Huffman, H.M.; Eaton, M.; Oliver, G.D. The Heat Capacities, Heats of Transition, Heats of Fusion and Entropies of Cyclopentene and Cyclohexene. *J. Am. Chem. Soc.* **1948**, *70*, 2911–2914. [CrossRef]
44. Douslin, D.R.; Huffman, H.M. The Heat Capacities, Heats of Transition, Heats of Fusion and Entropies of Cyclopentane, Methylcyclopentane and Methylcyclohexane 1. *J. Am. Chem. Soc.* **1946**, *68*, 173–176. [CrossRef]
45. Stull, D.R.; Sinke, G.C.; McDonald, R.A.; Hatton, W.E.; Hildebrand, D.L. Thermodynamic Properties of Indane and Indene. *Pure Appl. Chem.* **1961**, *2*, 315–322. [CrossRef]
46. Finke, H.; McCullough, J.; Messerly, J.; Osborn, A.; Douslin, D. Cis- and Trans-Hexahydroindan. Chemical Thermodynamic Properties and Isomerization Equilibrium. *J. Chem. Thermodyn.* **1972**, *4*, 477–494. [CrossRef]
47. Verevkin, S.P.; Samarov, A.A.; Vostrikov, S.V.; Wasserscheid, P.; Müller, K. Comprehensive Thermodynamic Study of Alkyl-Cyclohexanes as Liquid Organic Hydrogen Carriers Motifs. *Hydrogen* **2023**, *4*, 42–59. [CrossRef]
48. Müller, K.; Völkl, J.; Arlt, W. Thermodynamic Evaluation of Potential Organic Hydrogen Carriers. *Energy Technol.* **2013**, *1*, 20–24. [CrossRef]